

Diffractive Higgs Production by AdS Pomeron Fusion

Richard C. Brower ^{*}, Marko Djurić [†] and Chung-I Tan [‡]

August 30, 2018

Abstract

The double diffractive Higgs production at central rapidity is formulated in terms of the fusion of two AdS gravitons/Pomerons first introduced by Brower, Polchinski, Strassler and Tan in elastic scattering. Here we propose a simple self-consistent holographic framework capable of providing phenomenologically compelling estimates of diffractive cross sections at the LHC. As in the traditional weak coupling approach, we anticipate that several phenomenological parameters must be tested and calibrated through factorization for a self-consistent description of other diffractive process such as total cross sections, deep inelastic scattering and heavy quark production in the central region.

^{*}Physics Department, Boston University, Boston MA 02215

[†]Centro de Física do Porto, Departamento de Física e Astronomia, Faculdade de Ciências da Universidade do Porto, 4169-007 Porto, Portugal

[‡]Physics Department, Brown University, Providence, RI 02912

Contents

1	Introduction	3
2	Holographic Model for Diffractive Higgs Production	9
3	Kinematics and Regge Analysis of Building Blocks	15
3.1	Elastic Diffractive Scattering	15
3.2	Double Regge Analysis	17
4	Pomeron-Pomeron fusion Vertex	20
4.1	Higgs Vertex	20
4.2	Pomeron-Pomeron-Glueball Vertex	21
4.3	Higgs Production and Bulk to Boundary Propagator	23
5	Strategy for Phenomenological Estimates	26
5.1	Continuation to Tensor Glueball Pole and On-Shell Higgs Coupling	26
5.2	Normalization of the Glueball Form Factor	28
5.3	Near-Forward limit	31
5.4	First Estimate for Double-Pomeron Contribution	32
6	Summary and Discussion	37
A	AdS QCD and Conformal Symmetry Breaking	48

1 Introduction

A promising method for studying the Higgs meson at the LHC involves exclusive double diffractive Higgs production in forward proton-proton scattering. The protons scatter through very small angles with large rapidity gaps separating the Higgs in the central region,

$$p(k_1) + p(k_2) \rightarrow p(k_3) + H(q) + p(k_4) . \quad (1.1)$$

The Higgs subsequently decays into large transverse momentum fragments. Although this represents a small fraction of the total cross section, the exclusive channel should provide an exceptional signal to background discrimination by constraining the Higgs mass both to the energy of decay fragments and to the energy lost to the forward protons [1]. Relaxing the kinematics to allow for inclusive double diffraction may also be useful, where one or both of the nucleons are diffractively excited; we will defer these extensions to future studies. While double diffraction is very unlikely to be a discovery channel, it may play a useful role in determining properties of the Higgs when and if it is found.

Current phenomenological estimates of the diffractive Higgs production cross section have generally followed two approaches: perturbative (weak coupling) vs confining (strong coupling), or equivalently, in the Regge literature, often referred to as the “hard Pomeron” vs “soft Pomeron” methods. Previous works on diffractive Higgs production include [1, 2, 3, 4, 5, 6, 7, 8, 9, 10] (see for example [4] for additional related references). The Regge approach to high energy scattering, although well motivated phenomenologically, has suffered in the past by the lack of a precise theoretical underpinning. The advent of AdS/CFT has changed the situation. In a holographic approach, the Pomeron is a well-defined theoretical concept. The bare Pomeron is the leading planar term in the $1/N_c$ expansion at fixed 't Hooft coupling ($\lambda \equiv g^2 N_c$) which is then identified as the “AdS graviton” in the strong coupling [11] limit ($\lambda \rightarrow \infty$).

In this paper, we apply String/Gauge Duality to double diffractive Higgs production at central rapidity, formulated in terms of the fusion of two gravitons/Pomerons, first introduced by Brower, Polchinski, Strassler and Tan (BPST) in [11]. High energy diffractive collisions already have a rather extensive AdS/CFT literature to draw on. A key observation is **AdS-transverse factorization** that emerges at high energy as a *universal* feature, applicable to scattering involving both particles and currents. This leads to an AdS/Reggeon formulation with a few crucial phenomenological parameters which need to be fixed experimentally. Consequently using the *AdS* factorization and by comparing different processes the parameters are overconstrained allowing one both to test the accuracy of the framework and to give confidence to prediction when extended to new cross sections such as diffractive Higgs production. A semi-

nal paper by Strassler and Polchinski on deep inelastic scattering [12] already introduced some of the results later elaborated in Ref. [11] for elastic scattering. For instance, for elastic scattering, the amplitude can be represented schematically in a factorizable form (see Eq. (2.5)),

$$A(s, t) = \Phi_{13}(t) * \tilde{\mathcal{K}}_P(s, t) * \Phi_{24}(t) , \quad (1.2)$$

where the impact factors Φ_{13} and Φ_{24} represent two elastic vertex couplings to the external particles, and $\tilde{\mathcal{K}}_P$ is an universal BPST Pomeron kernel ¹, with a characteristic power behavior at large $s \gg |t|$,

$$\tilde{\mathcal{K}}_P \sim s^{j_0} . \quad (1.3)$$

This ‘‘Pomeron intercept’’, j_0 , lies in the range $1 < j_0 < 2$ and is a function of the ’t Hooft coupling, $g^2 N_c$. The $*$ -operator is defined explicitly by Eq. (2.5) in Sec. 2 below, with the kernel expressed more explicitly as $\tilde{\mathcal{K}}_P(s, t, z, z')$. It represents a convolution in the radial coordinate in AdS or more generally, in geometric terms, a 3-d convolution in transverse space, (\mathbf{x}_\perp, z) , combining the conventional impact parameter \mathbf{x}_\perp , conjugate to \mathbf{k}_\perp , and a 3rd radial coordinate, $r \sim 1/z$ of AdS^5 . There is also an extensive literature on eikonal sum in AdS space [13, 14, 15, 16, 17, 18]. In a recent paper by Brower, Djurić, Sarčević and Tan, this approach is applied to give a reasonable account of the small- x contribution to deep inelastic scattering [19]. Here one makes use of the universality property, Eq. (1.2). In moving from elastic to DIS, one simply replaces Φ_{13} in (1.2) by appropriate product of propagators for external currents [12, 19]. The same formalism can be applied as well to deeply virtual Compton scattering at small- x , as done recently by Costa and Djurić [20] ².

By virtue of factorization in AdS space, the extension to double diffractive Higgs production amplitude takes the form of

$$A(s, s_1, s_2, t_1, t_2) = \Phi_{13}(t_1) * \tilde{\mathcal{K}}_P(t_1, s_1) * V_H(s_1 s_2 / s, t_1, t_2) * \tilde{\mathcal{K}}_P(s_2, t_2) * \Phi_{24}(t_2) . \quad (1.4)$$

where we introduce the vertex V_H for the Pomeron fusion to Higgs processes. (See Eq. (3.16) for the explicit form.) Thus diffractive Higgs production requires three building blocks: Two from elastic scattering, the proton impact factors, Φ_{ij} and the Pomeron kernel (or Reggeon propagators), $\tilde{\mathcal{K}}_P$ and a new one for Pomeron-Pomeron-Higgs vertex V_H . Again in a self consistent holographic approach to high energy scattering, one must work at large but finite λ where the Pomeron intercept is of the order $j_0 \simeq 1.3$. As in the case of elastic scattering, the vertices will be evaluated at $\lambda = \infty$, unchanged from that calculated in the supergravity limit. An explicit form for this amplitude will be given in Sec. 4.3. Here we focus on understanding the new

¹Unlike the case of a graviton exchange in AdS , this Pomeron kernel contains both real and imaginary parts.

²The factorized form of the amplitude in AdS , but without the explicit form of the Pomeron kernel, has also been applied to a subset of DIS data in [21, 22].

vertex for Pomeron-Pomeron-Higgs fusion. However a critical issue not address is the proton impact factors coupling to the Pomeron kernel. Instead we assume a crude phenomenological modification of AdS wave function for a typical glueball state as discussed in Sec. 5. For example we have found a surprisingly good fits to HERA data for DIS at small x by approximating the proton as fixed wave-function at the IR boundary. We anticipate the need to study this more seriously in the context of global fits to many diffractive processes that are more sensitive probes of this AdS proton-proton-Pomeron vertex but it may well be that to a first approximation that the proton as seen by the Pomeron at large N_c does appear to be very much like a spherical glueball.

The key to our diffractive Higgs analysis is the recognition that, after integrating out the heavy quark loop, an external Higgs field couples effectively to the gluon Lagrangian density, $Tr[F^2]$, which by the AdS/CFT correspondence is the source of the dilaton field at the boundary of AdS space. Two particularly useful papers for our diffractive Higgs analysis are one by Herzog, Paik, Strassler and Thompson [23] on holographic double diffractive production of the scalar glueball and a second by Hong, Yoon and Strassler [24, 25] on the AdS/CFT vector form factor. We will show that the double-diffractive Higgs production vertex, V_H , essentially involves Pomeron-Pomeron fusion producing a dilaton in the bulk of AdS which propagates to the boundary via time-like AdS scalar form factor. However for this mechanism to work an important new feature in double diffractive Higgs production, not emphasized in [23], is the need for conformal breaking in the bulk of the AdS space. Without this conformal breaking in the bulk, the leading order Pomeron-Pomeron dilaton vertex would vanish. Of course QCD is not a scale invariant theory so any model of AdS/QCD must include some deformation of the AdS geometry. When scale invariance is broken, one expects a non-vanishing vev for the gluon Lagrangian density, F^2 . More generally, we will be interested in correlators involving a single F^2 , together with any number of stress-energy tensor $T_{\mu\nu}$, e.g., $\langle F^2(x)T_{\mu\nu}(y)T_{\mu\nu}(y') \dots \rangle$. These correlators can be evaluated at strong coupling through the use of Witten diagrams involving the graviton-graviton-dilaton coupling in the bulk. In a strictly conformal theory, scale invariance holds and all these correlators would vanish, corresponding to having a vanishing graviton-graviton-dilaton vertex in the bulk. This would in turn lead to a vanishing Higgs production vertex, $V_H = 0$. That is, under such a scenario, central double-diffractive Higgs production would be suppressed at high energy.

Symmetry breaking effect in AdS/CFT correspondence has been studied in the past mostly using a near-boundary analysis [26, 27, 28, 29, 30, 31, 32]. For our present purpose, it is more profitable to address scale invariance breaking in terms of Witten diagrams in the bulk. The simplest model, which we will use as a first approximation, is to terminate the space in the

IR (small radial co-ordinate r) at a hardwall for confinement. The normalizable modes are now discrete, giving rise to a glueball spectrum [33]. However since the bulk metric is unaffected, scale breaking effects resides on the IR wall only; for a non-vanishing graviton-graviton-dilaton coupling in the bulk, a second *ad hoc* conformal breaking mass parameter must be introduced. This is not completely surprising due to the lack of a self-consistent string dual for $N_c = \infty$ QCD. Fortunately it is possible to fix the overall Pomeron-Pomeron-dilaton coupling by appealing to the AdS/CFT dictionary. In the gauge description, it is fixed in terms of glueball matrix element of the trace of the energy momentum tensor, following the argument of Kharzeev and Levin [1] as explained in Sec. 5.2 and also in Appendix A. This matching condition between strong coupling and weak coupling is the best we can do in lieu of solution to long sought dual string to large N_c QCD.

With the advent of the AdS/CFT correspondence, we are now able to understand diffractive Higgs production starting from the extreme strong coupling limit. In a sense our approach is closer to production by the soft Pomeron, which is also an intrinsically non-perturbative treatment, used extensively by Donnachie and Landshoff and others to parametrize high energy diffractive hadronic process [34, 35, 36]. However holographic dual picture has the advantage of a unified soft and hard diffractive mechanism. In the extreme strong coupling limit the AdS/CFT dictionary maps gauge theory into classical gravity in Anti-de Sitter space. The leading correction to the strong coupling singularity [11, 13, 14] for the the $\mathcal{N} = 4$ Super Yang Mills is at

$$j_0(\lambda) = 2 - 2/\sqrt{g^2 N_c} , \quad (1.5)$$

moving down from the bare graviton at $J = 2$, Fig. 1(b), where $\lambda = g^2 N_c$. Comparing with weak coupling, we note that in weak coupling it starts instead as the two gluon exchange at $J = 2 - 1 = 1$ at $\lambda = 0$, Fig. 1(a), and summing the BFKL ladder moves to

$$j_0(\lambda) = 1 + (\ln 2/\pi^2) g^2 N_c \quad (1.6)$$

to first order [37, 38, 39, 40]. To this order both weak and strong calculation are consequences of a leading order in $1/N_c$ and conformal approximation to Yang Mills theory. Phenomenology for high energy cross sections suggest $j_0 \simeq 1.3$ for the bare Pomeron intercept, squarely in the cross over region suggesting both weak and strong coupling method may be useful to developing a reliable phenomenological ansatz for diffractive scattering in QCD.

We restrict ourselves in this paper primarily to the formulation of the holographic amplitude with a detailed analysis of the Pomeron-Pomeron Higgs production vertex in a dual approach with scale invariance breaking. We discuss methods for developing a phenomenology which allows the inclusion of the eikonal corrections as well as the calibration by other diffrac-

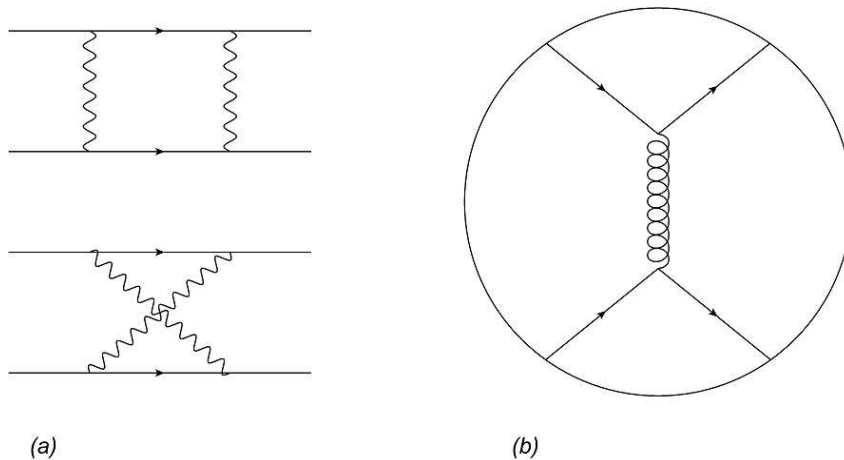


Figure 1: Comparison between the extreme weak and strong coupling Pomeron: (a) the 2 gluon exchange Low-Nussinov Pomeron at $g^2 N_c = 0$ with intercept $j_0 = 1$ and (b) the extreme strong coupling Witten diagram of AdS-graviton “Pomeron” at $g^2 N_c = \infty$ with intercept $j_0 = 2$.

tive processes for elastic scattering, deep inelastic scattering and $t\bar{t}$ production. This is not a full phenomenological analysis but a first critical ingredient. In a subsequent paper, we will use this formalism to perform a self-consistent analysis of elastic diffractive scattering, deep inelastic scattering and central diffractive heavy quark jets. Just as in a more conventional weak coupling perturbative approach, these will be required to constrain the parameters in the proton impact factors (or unintegrated gluon parton distributions), and the Higgs diffractive vertex [41]. Although encouraging studies of baryons in holographic QCD have been carried out [42, 43, 44, 45, 46], reliable calculations for meson- and nucleon-Pomeron vertex functions remain elusive. Full *ab initio* calculations are simply not possible at present even in the $1/N_c$ expansion due to the lack of precise AdS dual to QCD. Instead we must model properties of QCD by deforming the AdS^5 background metric to model the non-conformal consequences of confinement and asymptotic freedom. Nonetheless consistency with a full range of diffractive amplitudes is expected to lead to increasingly useful predictions.

This paper is organized as follows. In Sec 2, we give a narrative for diffractive scattering and double diffractive Higgs production from the AdS/CFT strong coupling view point. The goal is to itemize the assumptions leading to our analysis. In Sec. 3, we review the kinematics in the diffractive high energy limit and give details on the building blocks required to develop a model for holographic description of diffractive Higgs production. Sec. 4 deals with the kinematic aspects of the new vertex V_H for Pomeron-Pomeron fusion into the dilaton, while leaving to Appendix A a more detailed discussion on models with confinement deformation required

for scale invariance breaking and for double-diffractive Higgs production. Sec. 5 presents the normalization of double Pomeron Higgs production amplitude by extrapolation to the tensor glueball on the Pomeron trajectory. This in principle completes the specification of the Higgs production amplitude, (4.25). In Sec. 5.4, we provide a phenomenological treatment under a simple-pole approximation, leading to an estimate for the central diffraction Higgs production cross section of $.8 \sim 1.2$ pbarn. This is an over-estimate since it is arrived at without taking into account the absorptive correction, e.g., “survival probability”, which can lead to a central production cross section in the femtobarn range. In Sec 6, we conclude with comments on this and further corrections needed to make a more reliable prediction.

2 Holographic Model for Diffractive Higgs Production

Diffractive scattering and the notion of a Pomeron has always been an elusive object in QCD, often defined in a circular fashion as that which dominates high energy hadronic scattering. In the large N_c limit, there is a more precise definition of the “bare Pomeron”. In leading order of the $1/N_c$ expansion at fixed 't Hooft coupling $\lambda = g^2 N_c$, diffraction is given perturbatively by the exchange of a network of gluons with the topology of a cylinder, corresponding in a confining theory to the t-channel exchange of closed strings for glueball states. Unitarity imposes correction to the “bare Pomeron” in higher order in $1/N_c$: (i) by adding closed quark loops to the cylinder, leading to $q\bar{q}$ pairs or multi-hadron production via the optical theorem dominated by low mass pions, kaon etc and (ii) by multiple exchange of the Pomeron which includes the eikonal corrections (or survival probability) and triple-Pomeron and higher order corrections in a Reggeon calculus etc. As discussed in the Introduction, the advent of the AdS/CFT correspondence has provided a firm framework for a non-perturbative treatment.

To arrive at a picture of the bare Pomeron it is useful to consider its form in both weak and strong coupling. Diffractive scattering in QCD has been explored extensively in the past from a perturbative approach, where, in the lowest order, it can be modeled as color singlet two-gluon exchange (or Low-Nussinov Pomeron) given in Fig. 1a and later as a two Reggeized gluon ladder diagram (or the BFKL Pomeron) to first order in the 't Hooft coupling $g^2 N_c$ and all orders $g^2 N_c \log(s)$, with a BFKL intercept j_0 above unity given by (1.6). An elastic amplitude $A(s, t)$ now grows with a non-integer power as s^{j_0} , at t fixed.

While the use of Regge poles to model the Pomeron of non-perturbative QCD has a long history, a more mathematically explicit picture arises with the conjecture by Maldacena of an exact equivalence between IIB super string theory on $AdS_5 \times S_5$ and $\mathcal{N} = 4$ SUSY Yang Mills theory that holds true for all N_c at fixed λ . The $1/N_c$ expansion is string perturbation theory. We presume (or hope) that this string/gauge duality also holds for pure Yang Mills theory (i.e. QCD) although no construction has been found. Thus the bare Pomeron is the cylinder or closed string of the dual string. In practice detailed calculation are based leading order at large N_c and fixed 't Hooft coupling $\lambda = g^2 N_c$ which maps planar Yang Mills theory to a free closed string theory, followed by a strong coupling expansion $\lambda \rightarrow \infty$ which reduces the strings to point like object for the classical solution of supergravity in an AdS like background.

It is instructive to plot the Pomeron intercept $j_0(\lambda)$ for both strong and weak coupling as we have in Fig. 2 below. Perhaps it is an accident but the intersection of the strong coupling curve in Fig. 2 and the BFKL intercept to second order occurs near to the phenomenological

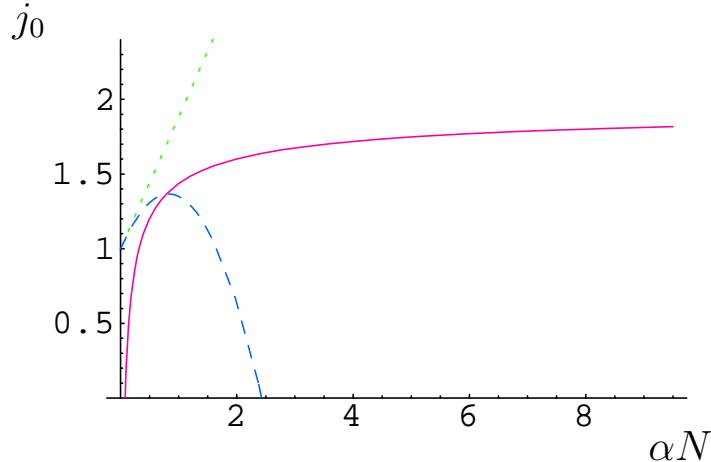


Figure 2: In $\mathcal{N} = 4$ Yang-Mills theory, the weak- and strong-coupling calculations of the position j_0 of the leading singularity for $t \leq 0$, as a function of $\alpha N = g^2 N_c / 4\pi$. Shown are the leading-order BFKL calculation (dotted), the next-to-leading-order calculation (dashed), and the strong-coupling calculation of this paper (solid). Note the latter two can be reasonably interpolated.

estimates, $j_0 \simeq 1.3$, of the intercept for QCD, suggesting that *the physics of diffractive scattering is roughly in the cross over region between strong and weak coupling*.

We conclude this section with a few remarks on the framework we are using to develop our strong coupling AdS/QCD model of diffraction. Readers familiar with holographic QCD models may wish to skip this recapitulation.

- AdS Gravity and Confinement:

In order to provide a particle interpretation, the basic framework for us is the holographic approximation to dual QCD with confinement deformation [47, 48, 49, 50, 51, 52]. At infinitely strong 't Hooft coupling, $g^2 N_c \rightarrow \infty$, the dual description,

$$S = \frac{1}{2\kappa^2} \int d^5x \sqrt{g} \left[-\mathcal{R} - V(\phi) + \frac{1}{2} g^{MN} \partial_M \phi \partial_N \phi + \dots \right], \quad (2.1)$$

is assumed to be 5d gravity coupled to dilaton field with a classical vacuum approximated by $AdS_5 \times Y_5$ geometry in the bulk. In principle we should solve the classical equation to define the background metric,

$$ds^2 = e^{2A(z)} [-dx^+ dx^- + dx_\perp dx_\perp + dz dz] + ds^2(Y^5) \quad (2.2)$$

Once the background geometry is known, expanding the action S to quadratic order in metric fluctuation h_{MN} , the graviton kernel, $\tilde{\mathcal{K}}_G$, can be found, (see (3.3) for an explicit representation.).

Of course there is no completely satisfactory example for such a background for QCD even at large N_c . Fortunately for high energy Higgs production the dominant fluctuations are the graviton/Pomeron field and dilaton that couples to the Higgs at the boundary which are less sensitive to the details of confinement deformation. The ellipsis in (2.1) represents other fields or branes from unknown short distances physics that survive the strong coupling limit. For example, for the $\mathcal{N} = 4$ Super Yang Mills, the pure $AdS_5 \times S_5$, background ($\exp[2A(z)] = R^2/z^2$), requires a 5-form Ramond-Ramond flux in order to introduce the cosmological constant

$$V(\phi) = -\frac{12}{R^2} . \quad (2.3)$$

At lower energy additional fields are needed, e.g., the Kalb-Ramond $B_{\mu\nu}$ field is required for the $C = -1$ odderon as noted in Ref. [33].

With confinement deformation, the AdS space is effectively cutoff in the interior. Because of the “cavity effect”, both dilaton and the transverse-traceless metric become massive, leading to an infinite set of massive scalar and tensor glueballs respectively. In particular, each glueball state can be described by a normalizable wave function $\Phi(z)$ in AdS . The weight factor Φ_{ij} in the respective factorized representation for the elastic and Higgs amplitudes, (1.2) and (1.4), is given by $\Phi_{ij}(z) = e^{-2A(z)}\Phi_i(z)\Phi_j(z)$. In contrast, for amplitudes involving external currents, e.g., for DIS [12, 19], non-normalizable wave-functions will be used.

- Correction to Strong Coupling in $1/\sqrt{\lambda}$:

As pointed out earlier, taking into account $O(1/\sqrt{\lambda})$ correction to the Graviton kernel, $\tilde{\mathcal{K}}_G$, one arrives at (1.2) and (1.4) for elastic and diffractive Higgs production respectively. Here the Pomeron kernel, $\tilde{\mathcal{K}}_P$, given explicitly in a J -plane representation, (3.3), has hard components due to near conformality in the UV and soft Regge behavior in the IR. We stress that this first order strong coupling correction corresponds to a stringy effect, as has been demonstrated in [11] by introducing a Pomeron world-sheet vertex operator \mathcal{V}_P while enforcing the on-shell condition,

$$(L_0 - 1)\mathcal{V}_P = (\bar{L}_0 - 1)\mathcal{V}_P = 0 . \quad (2.4)$$

As discussed in Ref. [33], this can also be carried out for the anti-symmetric field $B_{\mu\nu}$, leading to a description for Odderon in the strong coupling limit.

It is worth repeating that the importance of this stringy correction enters most importantly in the modification of the s -dependence of the Pomeron kernel, $\tilde{\mathcal{K}}_P$, with j_0 moving from 2 to a phenomenological value close to 1.3. However, for wave-function in (1.2) and (1.4), stringy corrections can be ignored. With this understanding, the 2-to-2 glueball scattering amplitude, (1.2), written in terms of AdS radial coordinate, becomes

$$A(s, t) = \int dzdz' \sqrt{-g(z)}\sqrt{-g(z')} \Phi_{13}(t, z)\tilde{\mathcal{K}}_P(s, t, z, z')\Phi_{24}(t, z'), \quad (2.5)$$

A more explicit form for the Pomeron kernel will be given in Appendix A.

- Weak Coupling Higgs Production:

In a perturbative approach, often dubbed as “hard Pomeron”, Higgs production can be viewed as gluon fusion in the central rapidity region [53]. A Higgs can be produced at central rapidity by the double Regge Higgs vertex through a heavy quark loop which in lowest order is a simple gluon fusion process as illustrated in Fig. 3a dominant for large parton x for the colliding gluons. A more elaborate picture emerges as one tries to go to the region of the softer (wee gluons) building up double Regge regime. In addition to the Pomeron exchange contribution in these models must subsequently be reduced by large Sudakov correction at the Higgs vertex and by so-called survival probability estimates for soft gluon emission, not inconsistent with the view of some that double diffractive Higgs production should be intrinsically non-perturbative.

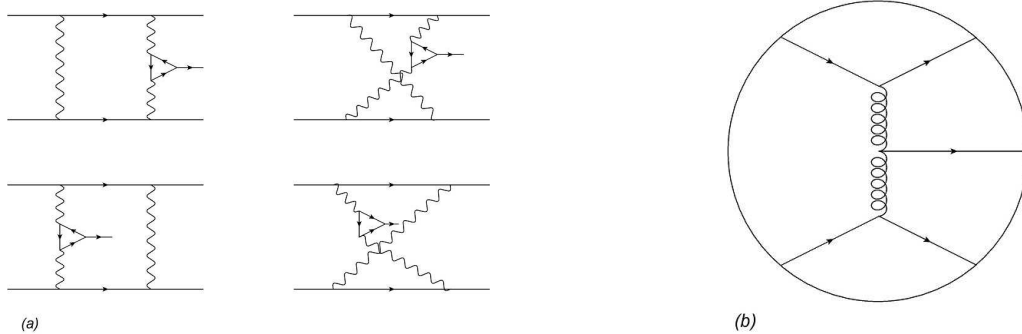


Figure 3: (a) Higgs production by gluon fusion in the 2 gluon exchange Low-Nussinov Pomeron at $g^2 N_c \rightarrow 0$ vs (b) The Witten diagram for Higgs production by AdS graviton fusion at $1/g^2 N_c \rightarrow 0$. The graviton fusion is a source of a bulk to boundary scalar the propagator for the heavy quark loop at the boundary.

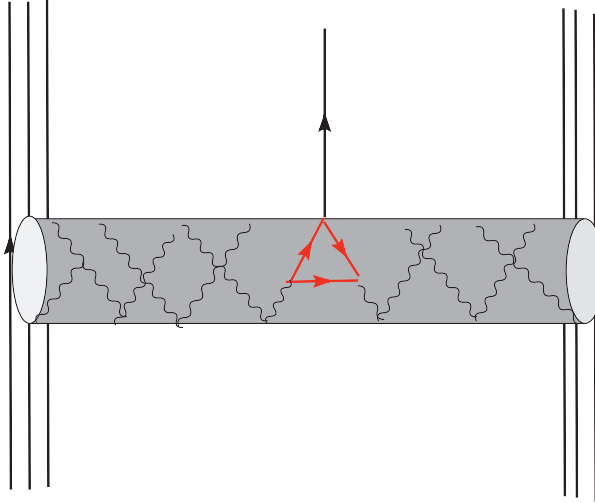


Figure 4: Cylinder Diagram for large N_c Higgs Production.

- Strong Coupling Higgs Production:

In the large N_c there are no quark loop in the bulk of AdS space and since the Higgs in the Standard Model only couples to quarks via the Yukawa interactions there appears to be a problem with strong coupling Higgs production in leading $1/N_c$. Fortunately the solution to this is to follow the standard procedure in Higgs phenomenology, which is to integrate out the quark field replacing the Higgs coupling to the gauge operator $Tr[F^2]$.

Consider the Higgs coupling to quarks via a Yukawa coupling, and, for simplicity we will assume it is dominated by the top quark. We will be more explicit in the next Section, and simply note here that, after taking advantage of the scale separations between the QCD scale, i.e., the Higgs mass and the top quark mass, $\Lambda_{QCD} \ll m_H \ll 2m_t$, heavy quark decoupling allows one to replace the Yukawa coupling by an effective interaction,

$$\mathcal{L} = \frac{\alpha_s g}{24\pi M_W} F_{\mu\nu}^a F^{a\mu\nu} \phi_H \quad (2.6)$$

by evaluating the two gluon Higgs triangle graph in leading order $O(M_H/m_t)$. Now the AdS/CFT dictionary simply requires that this be the source in the UV of the AdS dilaton field. It follows, effectively, for Higgs production, we are required to work with a five-point amplitude, one of the external leg involves a scalar dilaton current coupling to $Tr[F^2]$. For diffractive Higgs production, in the supergravity limit, the Higgs vertex V_H is given by a two-graviton-dilaton coupling, Fig. 3b. After taking into account finite λ correction, the leading order diagram at large N_c can be schematically represented in Fig. 4, with each of the left- and right-cylinders representing a BPST Pomeron.

- Conformal Symmetry Breaking:

Of course QCD, even at $N_c = \infty$, is not a conformal theory. Conformal symmetry breaking (or “dimensional transmutation” in the colorful language of Sidney Coleman) is ultimately tied to confinement in the IR and asymptotic freedom in the UV. A true QCD dual (or QCD string theory) would require an infinite number of (higher spin) fields in the bulk representation to correspond to fluctuations in the yet undiscovered world-sheet string theory for QCD. All mass scales (for quarkless large N_c QCD) are related and the coupling $\lambda = g^2 N_c$ is not a free parameter. Fortunately at high energy, these details are non-essential. For our purposes an adequate phenomenological AdS dual to QCD requires only two features: (1) an IR deformation, which for simplicity we take as hard-wall cut-off beyond $z = 1/\Lambda_{QCD}$, to give confinement and a linear static quark potential at large distances and (2) a slow deformation in the UV ($z \rightarrow 0$) to model the logarithmic running for asymptotic freedom. Moreover scale breaking plays an even more essential role in the application to diffractive Higgs production. In leading order in strong coupling, Pomeron-Pomeron fusion proceeds through a graviton-graviton-dilaton vertex, which is lacking in AdS gravity action (2.1) if scale invariance is maintained. This is demonstrated more explicitly in Appendix A. This vertex, $M^2 \phi h_{\mu\nu} h^{\mu\nu}$, itself requires a scale breaking mass parameter. However we will show, based on the AdS/CFT dictionary, that this new mass parameter can be fixed by computing a matrix element of the trace of the energy momentum tensor for the tensor glueball on the Pomeron trajectory following the argument of Kharzeev and Levin [1]. The overall rate of Higgs production is not a free parameter of our AdS/QCD model. Still all strong coupling QCD duals to date fail to relate the IR confinement scale to the UV scale (or to λ) so a least one extra mass needs to be fixed phenomenologically.

3 Kinematics and Regge Analysis of Building Blocks

The natural coordinates for high energy scattering in warped AdS^5 space are given in the Poincare patch in lightcone coordinates,

$$ds^2 = e^{2A(z)}[-dx^+ dx^- + dx_\perp dx_\perp + dz dz] , \quad (3.1)$$

where the incoming particles are directed near to the light cones $x_\pm = x^0 \pm x^z \simeq 0$ and the transverse impact parameters are extended to 3-dimensions, $\mathbf{b} = (x_\perp, z) = (x_1, x_2, z)$, the traditional 2-d transverse space, $\mathbf{x}_\perp = (x_1, x_2)$, plus the “radial” coordinate $z = R^2/r$. Here we relate this picture to the standard Mandelstam coordinates for 2-to-2 and 2-to-3 amplitudes in the Regge limit. We also introduce the analytic J -plane where the AdS Pomeron kernels take their simplest form.

3.1 Elastic Diffractive Scattering

For high energy elastic (nucleon) scattering,

$$p(k_1) + p(k_2) \rightarrow p(k_3) + p(k_4) , \quad (3.2)$$

the exact connection between light-cone coordinates and Mandelstam invariants are simplest in the brick-wall frame where $\mathbf{k}_{1\perp} = -\mathbf{k}_{3\perp} = \mathbf{q}_\perp/2$. In terms of the total rapidity y , the invariants are $s = (k_1 + k_2)^2 \equiv 4m_\perp^2 \cosh y$, $m_\perp^2 = m^2 + \mathbf{q}_\perp^2$ and $t = (k_1 - k_3)^2 = -\mathbf{q}_\perp^2$. The two component transverse momentum vector $\mathbf{q}_\perp = (q_1, q_2)$ is the Fourier transform of the impact co-ordinates x^1, x^2 . In the super-gravity limit where $\lambda \rightarrow \infty$, the one-graviton diagram grows as s^2 , (see (A.8)), and the one-graviton kernel is given by

$$\tilde{\mathcal{K}}_G(s, t, z, z') = s^2 (zz'/R^2)^2 \tilde{G}_2(z, z', t) \quad (3.3)$$

where

$$\tilde{G}_2(z, z', t = -\mathbf{q}_\perp^2) = \int \frac{d^2 x_\perp}{4\pi^2} e^{i\mathbf{q}_\perp \cdot (\mathbf{x}_\perp - \mathbf{x}'_\perp)} G_2(z, z', \mathbf{x}_\perp - \mathbf{x}'_\perp) \quad (3.4)$$

In the conformal limit, \tilde{G}_2 is simply the “massless” AdS_5 propagator in a momentum representation, satisfying a simply differential equation

$$(-z\partial_z z\partial_z + 4 - z^2 t) \tilde{G}_2(z, z'; t) = z \delta(z - z') \quad (3.5)$$

At finite λ , it has been shown in Ref. [11] that, due to curvature of AdS, the effective spin of a graviton exchange is lowered from 2 to $j_0 = 2 - 2/\sqrt{\lambda}$. As such it is necessary to adopt a

J -plane formalism where the Pomeron kernel $\tilde{\mathcal{K}}_P$ is given by an inverse Mellin transform ³,

$$\tilde{\mathcal{K}}_P(s, t, z, z') = - \int_{-i\infty}^{i\infty} \frac{dj}{2\pi i} (\alpha' \hat{s})^j \frac{1 + e^{-i\pi j}}{\sin \pi j} \tilde{G}_j(t, z, z'). \quad (3.6)$$

with $\hat{s} = zz's/R^2$. When conformal invariance is maintained, $\tilde{G}_j(t, z, z')$ satisfies a J -dependent “massive” AdS_5 differential equation

$$\left(-z\partial_z z\partial_z + (2\sqrt{\lambda})(j - j_0) - z^2 t\right) \tilde{G}_j(z, z'; t) = z \delta(z - z') \quad (3.7)$$

We remind the reader that the Regge J -plane is the conjugate variable to the light-cone boost operator: $\hat{H} = M_{+-}$ which in principle provides an exact one to one map for amplitudes using the Laplace/Mellin transform. To accomplish this one must transform separately contributions from exchanges of definite charge conjugation, $C = \pm 1$, or, more precisely, Regge contributions with a definite signature. The leading singularities for $C = \pm 1$ are referred to as the Pomeron and Odderon [33] respectively. For the closed string theory these exchanges are associated with the graviton and Kalb-Ramond fields respectively [33]. Applying this analysis to the AdS Pomeron amplitude, as detailed in Ref. [11], the elastic amplitude at high energy can again be represented schematically in a factorized form, Eq. (1.2).

The salient new element of the Regge formulation in the AdS/CFT description is the extra radial (or 5th) coordinate ($z = R^2/r$). The variable conjugate to $\log(z/R)$ is ν , which, up to a constant shift, is the conformal dimension, which in turns allows an inverse-Mellin representation [11]. It follows from Eq. (3.7) above that conformal Pomeron at $t = 0$, in a double-Mellin representation, is a simple pole in the $J - \nu$ plane,

$$\tilde{G}_j(\nu, t = 0) \sim \frac{1}{(2\sqrt{\lambda})(j - j_0) + \nu^2} \quad (3.8)$$

For non-zero t the full expression is given Eq. (A.12) of Appendix A. The coordinate z plays the role of “virtuality” in the partonic language of Yang Mills theory. As explained in [13, 14, 15, 16, 17, 18], in the conformal limit, in an impact representation at high energy, it leads to a transverse AdS^3 (or 3-d Hyperbolic space H_3), and a corresponding simpler expression for the Pomeron kernel, (5.23).

³For ease of writing, we have introduced $\tilde{\mathcal{K}}_P$ in this paper, which is simply related to \mathcal{K}_P used in Refs. [11, 13, 14, 19] by an AdS factor $\tilde{\mathcal{K}}_P = e^{(2A(z)+2A(z'))}\mathcal{K}_P$. This notation is more convenient in order to accommodate the use of impact factor $\Phi_{ij} = e^{-2A}\Phi_i\Phi_j$. For simplicity, we have also used through out, for this purpose, $e^{-2A} = (z/R)^2$.

3.2 Double Regge Analysis

The Regge analysis for 2-to-3 amplitude follows the same path as for the elastic amplitude but is considerably more subtle. The double diffractive Higgs production amplitude, $A(s, s_1, s_2, t_1, t_2)$,

$$p(k_1) + p(k_2) \rightarrow p(k_3) + H(q) + p(k_4) \quad (3.9)$$

has 5 Mandelstam invariants. Again we can express the invariants, $s = (k_1 + k_2)^2$, $s_1 = (k_3 + q)^2$, $t_1 = (k_1 - k_3)^2$, $s_2 = (k_4 - q)^2$, $t_2 = (k_2 - k_4)^2$ in terms of light cone coordinates by choosing an appropriate frame:

$$\begin{aligned} k_1 &= (m_1 e^{y/2}, m_1 e^{-y/2}, 0_\perp) \quad , & k_2 &= (m_2 e^{-y/2}, m_2 e^{y/2}, 0_\perp) \\ k_3 &= (m_{3\perp} e^{y_3}, m_{3\perp} e^{-y_3}, -q_{1\perp}) \quad , & k_4 &= (m_{4\perp} e^{-y_4}, m_{4\perp} e^{y_4}, -q_{2\perp}) \end{aligned} \quad (3.10)$$

where the transverse mass is $m_\perp = m^2 + k_\perp^2$ for any on shell state $k_i^2 = m^2$. The momentum for the central particle, $q = k_1 + k_2 - k_3 - k_4$ be parametrized by $q = (m_{H\perp} e^{y_H}, m_{H\perp} e^{-y_H}, q_{H\perp})$ with transverse mass $m_{H\perp}$,

$$m_{H\perp}^2 = m_H^2 + q_\perp^2 . \quad (3.11)$$

The double Regge limit is $|y_3 - y_H| \sim \log(s_1) \rightarrow \infty$, $|y_4 + y_H| \sim \log(s_2) \rightarrow \infty$ at fixed momentum transfers $t_i \simeq -k_{i\perp}^2$ and \mathbf{q}_\perp^2 . In this limit, one also has $y_3 \simeq -y_4 \simeq y/2$. The Higgs momentum components are fixed by energy-momentum conservation, e.g.,

$$y_H = \frac{1}{2} [\log(s_1/s_2) - \log(m_{3\perp}/m_{4\perp})] . \quad (3.12)$$

The transverse mass is specified by the relation,

$$\kappa = \frac{s_1 s_2}{s} \simeq m_H^2 + q_\perp^2 = m_{H\perp}^2 , \quad (3.13)$$

referred to as the ‘‘kappa’’ variable for the Regge-Regge particle vertex, $V(t_1, t_2, \kappa)$. It is natural to introduce the two outgoing rapidity gaps separating the Higgs as

$$\Delta y_1 = y_3 - y_H \quad , \quad \Delta y_2 = y_4 + y_H . \quad (3.14)$$

The light-cone parametrization provides exact change of coordinates: $s, s_i, t_i \rightarrow \Delta y_i, q_{i\perp}^2$. The double diffractive production limit is characterized by small transverse momenta, $t_i \simeq -q_{i\perp}^2$ and large rapidity gaps, $\Delta y_1 \simeq \log(s_1/(m_{3\perp} m_{H\perp}))$ and $\Delta y_2 \simeq \log(s_2/(m_{4\perp} m_{H\perp}))$.

In the double Regge limit the only ‘‘ κ ’’ dependence occurs in the Regge-Regge Higgs vertex, $V(t_1, t_2, \kappa)$. Note also since $\kappa = m_H^2 + q_{1\perp}^2 + q_{2\perp}^2 + 2q_{1\perp} \cdot q_{2\perp}$, κ is solely responsible for the so-called Toller angular dependence in $q_{1\perp} \cdot q_{2\perp}$ between the two protons scattering planes

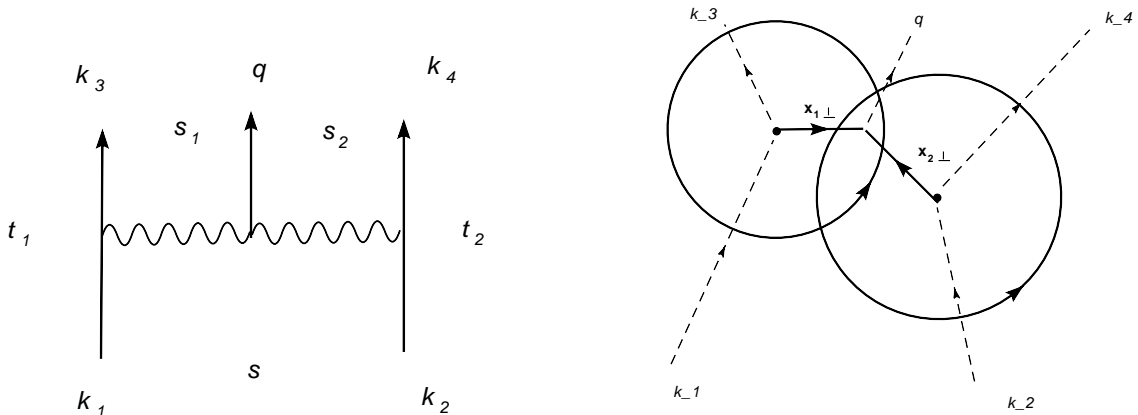


Figure 5: On the left the double Regge kinematics for $p(k_1) + p(k_2) \rightarrow p(k_3) + H(q) + p(k_4)$. At fixed center of mass energy \sqrt{s} , the final state configuration determined by 4 invariants t_1, s_1, t_2, s_2 . On the right, the impact parameter picture with the Higgs at $x_{H\perp}$ at a separations $\Delta x_{i\perp} = x_{H\perp} - x_{i\perp}$ of the two incoming particles. External momenta are for the \pm light-cone components only.

(see Fig. 5). The key to a double-Regge expansion is factorization in the J -plane. It is possible to obtain the full amplitude via a double-inverse-Mellin transform. We refer to the literature for further discussion of this formalism for some of the subtleties involved [54]. Most of these can be neglected due to the high mass of the Higgs at the central vertex. Consequently, with this *proviso*, we arrive at the amplitude for Higgs production expressed in terms of two Pomeron kernels, $\tilde{\mathcal{K}}_P(s_1, t_1, z_1, z'_1)$ and $\tilde{\mathcal{K}}_P(s_2, t_2, z'_2, z_2)$, together with a Higgs vertex, $V_H(t_1, t_2, \kappa, z'_1, z'_2)$. Finally we are able to give an explicit form to the symbolic expression for the double-Pomeron amplitude in Eq. 1.4 of the Introduction:

$$\begin{aligned}
A(s, s_1, s_2, t_1, t_2) &\simeq \int dz_1 dz'_1 dz'_2 dz_2 \sqrt{-g(z_1)} \sqrt{-g(z'_1)} \sqrt{-g(z'_2)} \sqrt{-g(z_2)} \\
&\times \Phi_{13}(t_1, z_1) \tilde{\mathcal{K}}_P(s_1, t_1, z_1, z'_1) V_H(t_1, t_2, \kappa, z'_1, z'_2) \tilde{\mathcal{K}}_P(s_2, t_2, z'_2, z_2) \Phi_{24}(t_2, z_2) .
\end{aligned} \tag{3.15}$$

In the above expression, impact factors, $\Phi_{13}(t_1, z_1)$ and $\Phi_{24}(t_2, z_2)$ are identical to those entering the elastic amplitude (2.5). This represents a generalization of Eq. (2.5) for elastic scattering to central diffractive Higgs production. The only new component is the Pomeron-Pomeron-Higgs vertex, $V_H(t_1, t_2, \kappa, z'_1, z'_2)$, which in general allows non-local interaction in AdS_3 , e.g., its dependence on z'_1 and z'_2 .

Just as the case of 2-to-2 scattering, it is often simpler to think of scattering in terms of transverse coordinates $\mathbf{b} = (x_\perp, z)$. Instead of the vertex $V_H(t_1, t_2, \kappa, z'_1, z'_2)$ in momentum

space, one can work directly with $V_H(x'_{1\perp} - x_{H\perp}, z'_1; x'_{2\perp} - x_{H\perp}, z'_2)$. The κ -dependence enters through the possible dependence on the angular correlation between the two proton's scattering planes, $x'_{1\perp} - x_{H\perp}$ and $x'_{2\perp} - x_{H\perp}$ or the scalar product: $(x'_{1\perp} - x_{H\perp}) \cdot (x'_{2\perp} - x_{H\perp})$. As we will see, for Higgs production, due to its large mass, this dependence is suppressed and we will choose to drop it. Indeed, (3.16) would take on a more complicated form if non-trivial $O(1/m_H^2)$ dependence on κ turns out to be important. We will not address this issue here.

4 Pomeron-Pomeron fusion Vertex

We now turn to a detailed discussion of the double diffractive Higgs vertex, V_H . So far our discussion of double-Pomeron exchange (1.4) applies equally well both to diffractive glueball production and to Higgs production. The situation is similar to how we converted the amplitude for proton-proton (p-p) elastic scattering to electron-proton deep-inelastic scattering (e-p DIS). For DIS, we simply replaced the normalizable proton wave-functions in (2.5) with non-normalizable counterparts appropriate for conserved external vector currents. For glueball production, the vertex is proportional to a normalizable AdS glueball wave-function, whereas for Higgs production, the vertex, V_H , requires a non-normalizable bulk-to-boundary propagator, $K(q^2, z)$, appropriate for a scalar external current. This section will explain how this transformation is done in detail.

4.1 Higgs Vertex

A Higgs scalar in the standard model [55, 56, 57, 58, 59] couples exclusively to the quarks via Yukawa coupling, which for simplicity we will assume is dominated by the top quark,

$$\mathcal{L} = -\frac{g}{2M_W} m_t \bar{t}(x)t(x)\phi_H(x) . \quad (4.1)$$

If we assume a mass for Higgs that obeys

$$\Lambda_{QCD} \ll m_H \ll 2m_t , \quad (4.2)$$

we can use the conventional heavy quark approximation [60] by integrating out the top quark loop replacing the Yukawa coupling by the effective coupling of Higgs field to the gluon operator,

$$\mathcal{L} = L(q^2)F_{\mu\nu}^a F^{a\mu\nu} \phi_H , \quad (4.3)$$

where

$$L_H \equiv L(-m_H^2) \simeq \frac{\alpha_s g}{24\pi M_W} , \quad (4.4)$$

to leading order $O(m_H/m_t)$. In the dual AdS description at leading order in $1/N_c$ heavy quarks are external sources near to the boundary of AdS so this procedure just replaces the source $\bar{t}(x)t(x)$ by $F^2(x)$ at the boundary. Consequently the vertex $V_H(x'_{1\perp} - x_{H\perp}, z'_1; x'_{2\perp} - x_{H\perp}, z'_2)$ is now given by the product of a Pomeron-Pomeron-dilaton vertex in the bulk and a scalar bulk-to-boundary propagator, $K(x'_H - x_H, z)$ from the interior of AdS_3 at $\mathbf{b}_H = (x'_H, z)$ to the source $F_{\mu\nu}^a F_{\mu\nu}^a(x)$ at $z_0 \rightarrow 0$. In the most general form, the Pomeron-Pomeron-dilaton vertex

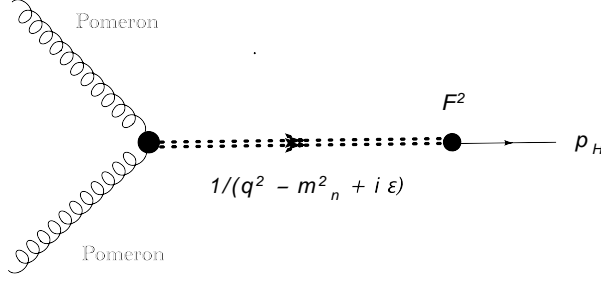


Figure 6: Factorization of double diffractive vertex in strong coupling: From right to left: $F^2(x)$ -Higgs vertex the boundary of AdS ($z_H = 0$), the boundary to scalar propagator saturated by glueballs and, finally, the double Pomeron to scalar vertex in the interior of AdS (z_0).

can be non-local where the two Pomerons “fuse” at z'_1, z'_2 into a dilaton at z . So our vertex would take the form,

$$V_H(t_1, t_2, \kappa, z'_1, z'_2) = L_H \int dz \mathcal{V}(t_1, t_2, \kappa, z'_1, z'_2, z) K(q^2, z), \quad (4.5)$$

evaluated on shell at $q^2 = -M_H^2$. However in the spirit of strong coupling, we impose locality on the Pomeron-Pomeron scalar vertex in the bulk,

$$\mathcal{V}(t_1, t_2, \kappa, z'_1, z'_2, z) = (1/\sqrt{-g}) \delta(z'_1 - z) \delta(z'_2 - z) \mathcal{V}_L(t_1, t_2, \kappa, z) \quad (4.6)$$

Therefore, the overall central Higgs vertex V_H can be written as a product of several factors,

$$V_H(t_1, t_2, \kappa, z, z'_2) = (1/\sqrt{-g}) \delta(z - z'_2) L_H \mathcal{V}_L(t_1, t_2, \kappa, z) K(q^2, z) \quad (4.7)$$

Of course this first step, taking the heavy quark limit, $m_H \ll m_t$, is simply the standard approximation often used in Higgs production for both soft and hard gluon fusion. We can achieve further simplifications by taking advantage of the fact that $\Lambda_{QCD} \ll m_H$. Before doing so, it is instructive to first re-consider the case of production of scalar glueballs.

4.2 Pomeron-Pomeron-Glueball Vertex

In a treatment with confinement deformation, the bulk-to-boundary propagator can be saturated by a set of scalar glueballs with increasing masses. The factorized structure, (4.7), can then be schematically represented by Fig. 6. It is therefore useful to first consider double diffraction vertex for scalar production of a massive glueball of mass m_n , $V_n(t_1, t_2, \kappa, z'_1, z'_2)$. Here κ is a

standard double-Regge invariant, $\kappa = s_1 s_2 / s$, which we will return to shortly. In momentum space, this vertex can be expressed as

$$V_n(t_1, t_2, \kappa, z'_1, z'_2) = \int dz \mathcal{V}_n(t_1, t_2, \kappa, z'_1, z'_2, z) \phi_n(z) \quad (4.8)$$

where we have labeled scalar glueballs by n , with a wave-function $\phi_n(z)$ in AdS and a coupling f_n to two Pomerons. As noted above, the coupling \mathcal{V} is in general non-local in AdS , depending on z'_1, z'_2, z . However, in the super-gravity limit, scattering becomes local, as schematically represented by the Witten diagram, Fig. 3b, i.e., $z'_1 = z'_2 = z$. In fact, in this limit, $\mathcal{V}_n(t_1, t_2, \kappa, z'_1, z'_2, z') \rightarrow \text{constant}$, leading to

$$V_n(t_1, t_2, \kappa, z'_1, z'_2) = \delta(z'_1 - z'_2) \mathcal{V}_n \int dz \delta(z'_1 - z) \phi_n(z) \quad (4.9)$$

However for λ finite, we should entertain non-trivial dependence on its arguments, at least consistent with that which is seen in flat-space string theory. But we can still assume locality in the AdS radial co-ordinate as advocated in Ref. [24], leading to

$$V_n(t_1, t_2, \kappa, z'_1, z'_2) \simeq \delta(z'_1 - z'_2) \int dz \delta(z'_1 - z) \mathcal{V}_n(t_1, t_2, \kappa, z) \phi_n(z). \quad (4.10)$$

In a double-Regge limit, κ is kinematically given by the transverse momentum by $\kappa = m_n^2 + q_\perp^2$. In a frame where incoming particles 1 and 2 are longitudinal, translation invariance leads to $q_\perp = -(q_{3\perp} + q_{4\perp})$ and rotational invariance then allows the vertex to depend only on magnitudes of $q_{3\perp}$ and $q_{4\perp}$, and on the relative angle between them, e.g., $|q_{3\perp}|$, $|q_{4\perp}|$, and their vector dot-product $q_{3\perp} \cdot q_{4\perp}$. Equivalently, since $\kappa = m_n^2 + q_\perp^2$, the vertex can also be considered as a functions of $t_1 = -q_{3\perp}^2$, $t_2 = -q_{4\perp}^2$, and q_\perp^2 . Therefore, $\mathcal{V}(t_1, t_2, \kappa, z')$ provides the most general information appropriate for local Pomeron fusion in AdS.

In flat space the dependence of $\mathcal{V}(t_1, t_2, \kappa, z)$ on t_1, t_2, κ has been studied extensively. For an arbitrary external particle with spin, the vertex will also have additional spin dependence. However, for our present purpose, we only need to consider scalar production, with its mass m_n^2 allowed to take on large values. Let us focus on the dependence of $\mathcal{V}_{flat}(t_1, t_2, \kappa)$ on the variable κ . The general analytic structure in κ is robust. For open-string, it is real for $\kappa < 0$, with branch cut along the positive real axis, $\kappa \geq 0$. At $\kappa = 0$, one has

$$\mathcal{V}_{flat}(t_1, t_2, \kappa) \simeq (-\kappa^{-1})^{\alpha_1} G_1 + (-\kappa^{-1})^{\alpha_2} G_2 \quad (4.11)$$

where G_1 and G_2 are regular at $\kappa = 0$. This analytic structure ⁴, (or Steimann relations), is required to avoid overlapping discontinuities not present in planar diagrams on the one hand

⁴For related recent studies, see [61] and references therein.

and in the Regge limit of open strings on the other. For closed strings, a similar analysis can also be carried out, with branch points at $\kappa = 0$ and at $\kappa = \infty$, extending to the entire real axis. Returning to the case of AdS , this singularity structure can play an important role for light glueball production, and this has been addressed in [24]. In particular, with κ^{-1} large, each of the two terms leads to separate “diffusion” effects. However, for our present purpose, this turns out to be less important. Indeed, from flat-space string theory, one finds that, in the limit $\kappa \rightarrow \infty$

$$\mathcal{V}_{flat}(t_1, t_2, \kappa) \rightarrow \kappa^{-2} \beta_0(t_1) \beta_0(t_2) \quad (4.12)$$

thus leading to a simplified structure. Furthermore, since $\kappa = q_\perp^2 + m_n^2$ for high-mass $\kappa \gg q_\perp^2$, the dependence on q_\perp^2 is effectively lost up to $O(q_\perp^2/m_n^2)$ corrections. In moving to impact space, we find that the vertex depends only on $x_2 = |x_{2\perp} - x_\perp|$ and $x_4 = |x_{4\perp} - x_\perp|$, and is independent of $x_{24} = |x_{2\perp} - x_{4\perp}|$. That is, for production of a heavy object, angular correlation between the left- and right-moving systems decouple, leading to a much simplified analytic structure. In what follows, for Higgs production, due to $\Lambda_{QCD} \ll m_H$, we drop the dependence on κ entirely.

With these considerations, we are led to a parametrization of the amplitude for a diffractive high-mass glueball production

$$A(s, s_1, s_2, t_1, t_2) = \Phi_{13} * \tilde{\mathcal{K}}_P * V_n * \tilde{\mathcal{K}}_P * \Phi_{24} . \quad (4.13)$$

where the production vertex, V_n , is local in AdS -radius, i.e.,

$$\begin{aligned} A(s, s_1, s_2, t_1, t_2) \simeq & \int dz_1 dz_2 dz_3 \sqrt{-g_1} \sqrt{-g} \sqrt{-g_2} \Phi_{13}(t_1, z_1) \tilde{\mathcal{K}}_P(s_1, t_1, z_1, z) \\ & \times V_n(t_1, t_2, z) \tilde{\mathcal{K}}_P(s_2, t_2, z, z_2) \Phi_{24}(t_2, z_2) . \end{aligned} \quad (4.14)$$

4.3 Higgs Production and Bulk to Boundary Propagator

Returning to the original problem, we now consider the coupling for the Pomeron fusion to an external source F^2 through the bulk to boundary propagator $K(x_\perp - x'_\perp, z)$. That is, we are calculating an amplitude involving a nonnormalizable wave function for the leg associated with the Higgs. Therefore, the amplitude involves one factor of the bulk-to-boundary propagator $K(q^2, z)$, in a momentum representation. Using $\Lambda_{QCD} \ll m_H$ we will show that the dominant contribution to the resulting integration over the AdS radius comes from

$$z \simeq O(1/M_H). \quad (4.15)$$

To see how this comes about, we need to evaluate the bulk to boundary propagator at $q^2 = -m_H^2$. This issue was studied in some detail by Hong, Yoon and Strassler [25] focused on the

vector current coupling to the tower of AdS glueballs. Here we are considering the scalar term in the energy-momentum current which is essentially a trivial modification. More difficult is understanding the analytic continuation to time-like momentum $q^2 = -m_H^2$.

Consider the hard wall model for a confining AdS/CFT for clarity at first. Following Ref. [25] the bulk to boundary propagator can be viewed as the non-normalizable wave function excited by the current (F^2 in our case) at the boundary:

$$\psi(q^2, z) = \sum_n \frac{f_n \phi_n(z)}{q^2 + m_n^2} \quad (4.16)$$

where the “decay constant” for the n-th glueball state, f_n , is

$$f_n = \langle 0 | F^2(x=0) | n, p \rangle \sim m_n^3 \quad (4.17)$$

for the nth scalar glueball with on-shell eigen solution, $\exp[ipx]\phi_n(z)$ for $p^2 = -m_n^2$. Since the bulk-to-boundary propagator is determined by the background geometry, the relative strengths of f_n are fixed.

In the conformal limit, scalar bulk-to-boundary propagator in a momentum presentation can be expressed explicitly is

$$K(z, q) = (qz)^2 K_2(qz) = z^2 \int_0^\infty \frac{dm m^3 J_2(mz)}{q^2 + m^2} = \int_0^\infty \frac{dx x^3 J_2(x)}{z^2 q^2 + x^2} . \quad (4.18)$$

where K_ν is the modified Bessel function. Note $(qz/2)^\nu K_\nu(qz) \simeq \Gamma(\nu)/2$ for small qz and $K_\nu(qz) \simeq \sqrt{\pi/(qz)} e^{-qz}$ for large $qz > 0$. It follows that, when averaged over smooth functions of z , integrals such as

$$I(q) = \int_0^\infty dz T(z) K(z, q) \sim T(1/q) \quad (4.19)$$

are dominated by the end-point region where $z = O(1/q)$ as was also the case for DIS ([19]).

In our current application to Higgs production, we also need to analytically continue to the region where q is time-like. Numerically we find this is a good approximation after analytical continuation to $-q^2 = (m_H + i\Gamma)^2$ or $q = im_H + \Gamma$. We note that we need to convolute this bulk-to-boundary propagator over products of two Pomeron Green’s functions, which will be smooth in z . For example at $t_1 = t_2 = 0$, the explicit expression, up to smooth logarithmic corrections, can be expressed as

$$V(m_H) \sim \pi(z_1 z_2)^2 \int_0^\infty \frac{dz}{z} e^{-izm_H - z\Gamma} e^{j_0(\tau_1 + \tau_2) - \ln^2(z/z_1)/(2 - j_0)\tau_1 - \ln^2(z/z_2)/(2 - j_0)\tau_2} \quad (4.20)$$

with $\tau_i = \ln(zz_i s_i)$. Note the dominant rapid oscillations due to the factor e^{-izM_H} and also a convergence factor $e^{-z\Gamma}$. (For confining situation, e.g., hard-wall, the z -integral is cutoff at large z .) It can be shown that the dominant contribution to the integral for large M_H comes again from $z \sim 1/m_H$. This can be seen by writing the integral as

$$(z_1 z_2)^2 \int_0^\infty dz \exp[-F(z)] \quad (4.21)$$

where

$$\begin{aligned} F(z) &= izm_H + z\Gamma - (2j_0 - 1) \ln(z) \\ &+ \ln^2(z/z_1)/((j_0 - 2) \ln(zz_1 s_1)) + \ln^2(z/z_2)/((j_0 - 2) \ln(zz_2 s_2)). \end{aligned} \quad (4.22)$$

For $s_1 = s_2 = O(\sqrt{s})$ large, the saddle point z^* is essentially determined by the first two terms on the right of (4.22), leading to

$$z^* \simeq (2j_0 - 1)/(im_H + \Gamma) \quad (4.23)$$

The validity of this approximation can also be verified numerically. Therefore as an approximate treatment, one can represent the bulk-to-boundary propagator by

$$K(x'_H - x_H, z') \sim \delta(x'_H - x_H) \delta(m_H z' - c) \quad (4.24)$$

where $c = O(1)$. We can further rescale z so that $c = 1$.

We are finally in the position to put all the pieces together. Although we eventually want to go to a coordinate representation in order to perform eikonal unitarization, certain simplification can be achieved more easily in working with the momentum representation. The Higgs production amplitude, schematically given by (1.4), can be written explicitly as

$$\begin{aligned} A(s, s_1, s_2, t_1, t_2) &\simeq \int dz_1 dz dz_2 \sqrt{-g_1} \sqrt{-g} \sqrt{-g_2} \Phi_{13}(z_1) \\ &\times \tilde{\mathcal{K}}_P(s_1, t_1, z_1, z) V_H(q^2, z) \tilde{\mathcal{K}}_P(s_2, t_2, z, z_2) \Phi_{24}(z_2). \end{aligned} \quad (4.25)$$

where $q^2 = -m_H^2$. For the production vertex, however, we will keep it simple by expressing it more generally as

$$V_H(q^2, z) = V_{PP\phi} K(q^2, z) L_H \quad (4.26)$$

where $K(q^2, z)$ is the conventionally normalized bulk to boundary propagator, $V_{PP\phi}$ serves as an overall coupling from two-Pomeron to F^2 , and L_H is the conversion factor from F^2 to Higgs. Treating the central vertex $V_{PP\phi}$ as a constant, which follows from the super-gravity limit, we have ignored possible additional dependence on κ , as well as that on t_1 and t_2 . This approximation gives an explicit factorizable form for Higgs production.

5 Strategy for Phenomenological Estimates

While the goal of this paper is simply to extend holographic diffraction to Higgs production, it is useful to outline the phenomenological approach we plan to pursue to confront experimental data. There should be a strong warning however that details will necessarily change as we discover which parametrization are critical to a global analysis of data. Our current version for the holographic Higgs amplitude involves 3 parameters: (1) the hardwall IR cut-off determined by the glueball mass, (2) the leading singularity in the J -plane determined ⁵ by the 't Hooft parameter $g^2 N_c$ and (3) the strength of the central vertex parametrized by the string coupling or Planck mass. A strategy must be provided for fixing these parameters. The glueball mass at large N_c can in principle be fixed by lattice QCD methods and the leading J -plane singularity from total cross section data. Finally the central vertex, V_H , or equivalently, $V_{PP\phi}$, via (4.26), can be normalized, following the approach of Kharzeev and Levin [1] based on the analysis of the trace anomaly. Since one can in principle use elastic scattering to normalize the bare BPST Pomeron coupling to external protons, once $V_{PP\phi}$ is known, the central Higgs production amplitude, (4.26), is completely determined. This procedure for determining this crucial overall scale deserves further explanation.

5.1 Continuation to Tensor Glueball Pole and On-Shell Higgs Coupling

Confinement deformation in AdS will lead to glueball states, e.g., the lowest tensor glueball state lying on the leading Pomeron trajectory [62]. There will also be scalar glueballs associated with the dilaton. With scalar invariance broken, this will also lead to non-vanishing couplings between a pair of tensor glueballs and scalar glueballs. When translated into a Witten diagrammatic description in the bulk, as we have also pointed out earlier, this leads to a non-vanishing graviton-graviton-dilaton coupling and in turn leads to $V_H \neq 0$.

Consider first the elastic amplitude. With confinement, each Pomeron kernel will contain a tensor glueball pole when t goes on-shell. Indeed, the propagator for our Pomeron kernel can be expressed as a discrete sum over pole contributions, i.e., Eq. (5.21). That is, when $t \simeq m_0^2$, where m_0 is the mass of the lightest tensor glueball, which lies on the leading Pomeron trajectory, i.e., $m_0^2 = m_0^2(j=2)$, we need only to keep the lowest term in (5.21), and the kernel takes on a factorizable form.

⁵Note that in a true dual to QCD at $N_c = \infty$ the only free parameter is a single mass scale that by “dimensional transmutation”, replaces the coupling constant and all dimensionless ratios. So only the first parameter would be needed phenomenologically.

It follows that the elastic amplitude, Eq. (2.5), when approaching the t -channel pole at $t = m_0^2$, is pole-dominated,

$$A(s, t) \simeq g_{13} \frac{s^2}{m_0^2 - t} g_{24} \quad (5.1)$$

with vertex g_{ij} given by an overlapping integral:

$$g_{ij}(m_0^2) = \alpha' \int dz \sqrt{-g(z)} e^{-4A(z)} \beta(m_0^2) \Phi_i(z) \Phi_j(z) \phi_G(z). \quad (5.2)$$

The tensor glueball wave function, for hard-wall model, is given by $\phi_G(z) = \tilde{\phi}_0(x, j = 2)$. Here, we have generalized Φ_{ij} as the product of two external wave functions, together with an extra factor $\beta(t)$, i.e., $\Phi_{ij}(t, z) = \beta(t) e^{-2A(z)} \Phi_i(z) \Phi_j(z)$, for phenomenological reasons. That is, the external coupling g_{ij} is given by an overlap-integral over a product of three wave functions, $\Phi_i(z)$, $\Phi_j(z)$ and $\phi_G(z)$, consistent with the discussion in [24, 25]. With the standard normalization, $A(s, t)$ is dimensionless, thus $g_{ij}(m_0^2)$ has the dimension of length.

Let us next turn to the Higgs production amplitude, Eq. (4.25). Note that the Pomeron kernel now appears twice, $\tilde{\mathcal{K}}_P(s_1, t_1, z_1, z)$ and $\tilde{\mathcal{K}}_P(s_2, t_2, z_2, z)$. When nearing the respective tensor poles at $t_1 \simeq m_0^2$ and $t_2 \simeq m_0^2$, we can again use the leading-pole approximation for the kernel, (5.28). The amplitude can now be expressed as

$$A(s, s_1, s_2, t_1, t_2) \simeq g_{13} \frac{\Gamma_{GGH} s^2}{(t_1 - m_0^2)(t_2 - m_0^2)} g_{24} \quad (5.3)$$

We have performed the z_1 and z_2 integrations as done for the elastic amplitude, leading to external coupling g_{13} and g_{24} respectively, given by (5.2), and also have made use of the fact that $s_1 s_2 \simeq \kappa s \simeq m_H^2 s$. Here Γ_{GGH} is the effective on-shell glueball-glueball-Higgs coupling, which can be written in terms of the central vertex, $V_{PP\phi}$.

Recall that, after integrating out the top quark, the effective on-shell glueball-glueball-Higgs coupling can be expressed as $\Gamma_{GGH} = L_H F(-m_H^2)$, with L_H given by (4.4) and

$$F(q^2) = (\alpha' m_H^2)^2 V_{PP\phi} \int dz \sqrt{-g(z)} e^{-4A(z)} \phi_G(z) K(q, z) \phi_G(z) \quad (5.4)$$

This follows from (4.25) and (4.26). Observe that, by going on-shell, F can be considered as a scalar form factor, where

$$F(q^2) = \langle G, ++, q_1 | F_{\mu\nu}^a F_{\mu\nu}^a(0) | G, --, q_2 \rangle \quad (5.5)$$

That is, in the high energy Regge limit, the dominant contribution comes from the maximum helicity glueball state [11], with $\lambda = 2$. Note that (5.4) is in the form of an integral over a product of the bulk-boundary propagator with other smooth functions, (4.19). In the large m_H

limit, the dominant contribution comes from $z = O(m_H^{-1})$. What remains to be specified is the overall normalization, $F(0)$, or equivalently the coupling $V_{PP\phi}$.

We also note in passing that the expression for this form factor is precisely what is expected from Eq. (A.6) since we are considering a situation with a constant Witten vertex, assuming no running⁶. Conformal scaling determines the large $Q^2 = |q^2|$ behavior to be $F_{GG}(q^2) \sim (1/Q)^{\Delta_1 + \Delta_2 - 4} = 1/Q^4$ with $\Delta_1 = \Delta_2 = \Delta_G = 4$, as can be readily checked. This form factor can also be written, using (4.16), as

$$F_{GG}(q^2) = (\alpha' q^2)^2 \sum_n \frac{g_{GG\varphi_n} f_n}{q^2 + m_n^2}, \quad (5.6)$$

which follows when we express the bulk-to-boundary propagator $K(q, z)$ in a dispersion sum over the dilaton scalars, with the coupling constants given by

$$g_{GG\varphi_n} = V_{PP\phi} \int dz \sqrt{-g(z)} e^{-4A(z)} \phi_G(z) \phi_n(z) \phi_G(z) \quad (5.7)$$

5.2 Normalization of the Glueball Form Factor

From the gauge theory view, we recognize that $F(q^2)$ at $q^2 = 0$, is a matrix element of the trace of the energy momentum tensor. So we can follow D. Kharzeev and E. M. Levin [1], who considered the matrix elements of the trace-anomaly between two states, $|\alpha(p)\rangle$ and $|\alpha'(p')\rangle$, with four-momentum transfer $q = p - p'$. In particular, for a single particle state of a tensor glueball $|G(p)\rangle$, this leads to $\langle G(p) | \Theta_\alpha^\alpha | G(p') \rangle = \frac{\tilde{\beta}}{2g} \langle G(p) | F_{\mu\nu}^a F^{a\mu\nu} | G(p') \rangle$. At $q = 0$, the forward matrix element of the trace of the energy-momentum tensor is given simply by the mass of the relevant tensor glueball, with $\langle G | \Theta_\alpha^\alpha | G \rangle = M_G^2$, this directly yields

$$F(0) = \langle G | F_{\mu\nu}^a F^{a\mu\nu} | G \rangle = -\frac{4\pi M_G^2}{3\tilde{\beta}} \quad (5.8)$$

where $\tilde{\beta} = -b\alpha_s/(2\pi)$, $b = 11 - 2n_f/3$, for $N_c = 3$. In what follows, we will use $n_f = 3$. Note that heavy quark contribution is not included in this limit. Since the conformal scale breaking is due to the running coupling constant in QCD, there is apparently a mapping between QCD scale breaking and breaking of the AdS background in the IR, which gives a finite mass to the glueball and to give a non-zero contribution to the gauge condensate.

We are now in the position to provide the proper normalization for $V_{PP\phi}$. It is convenient to formally define

$$\Gamma_{GGH}(q^2) \equiv \frac{\alpha_s g}{24\pi M_W} F(q^2) \quad (5.9)$$

⁶A more consistent treatment would be to adopt the precise coupling given by the model, (A.6). However, we will not follow this path in what follows.

It follows that the normalization at $q^2 = 0$ is given by

$$\Gamma_{GGH}(q^2 = 0) = \frac{\alpha_s g}{24\pi M_W} F(0) = \frac{2M_G^2}{3vb} = 2^{1/4} G_F^{1/2} \frac{2M_G^2}{27} \quad (5.10)$$

More explicitly, from (4.25) and (4.26), we have

$$V_{PP\phi} = C^{-1} L_H^{-1} (\alpha' m_H^2)^{-2} \Gamma_{GGH}(0) \quad (5.11)$$

where C is given by a finite integral

$$C = \int dz \sqrt{-g(z)} e^{-4A(z)} \phi_G(z) K(0, z) \phi_G(z) \quad (5.12)$$

and is $O(1)$.

It is worth recapitulating the key discussion in [1], which makes essential use of the scale anomaly. More generally, when quarks are massive, trace anomaly can be expressed as

$$\Theta_\alpha^\alpha = \frac{\tilde{\beta}}{2g} F^{\alpha\beta a} F_{\alpha\beta a} + \sum_{l=u,d,s} m_l \bar{q}_l q_l + \sum_{h=c,b,t} m_h \bar{q}_h q_h \quad (5.13)$$

where we have separated quarks into light and heavy. In (5.13), $\tilde{\beta}$ now includes contributions from all quarks, both light and heavy. In this case, scale invariance is broken explicitly by quark masses. In the heavy quark decoupling limit, it has been shown that the explicit contribution from the last term cancels the corresponding heavy quark contribution to the beta-function. For simplicity, consider also the situation where light quarks are massless. In this limit, $\tilde{\beta}$ receives contributions from gluons and light quarks only. Therefore, a proper heavy quark decoupling in (5.13) allows an identification of matrix element of $m_h \bar{q}_h q_h$ in the heavy quark limit with that of the corresponding matrix element of F^2 . This equivalence corresponds precisely to the mechanism for a central Higgs production discussed in Sec. 4.

Recall that Higgs couples directly to quark-antiquark pairs, Eq. (4.1), with a strength proportional to the quark mass. In practice, we will keep only the $t\bar{t}$ pair. In our earlier treatment, after taking into account the triangle graph, it converts this coupling to an effective local interaction directly with gluons through the combined effective Higgs production coupling where Higgs now couples directly to F^2 , going from (4.1) to (4.3). This conversion is achieved in the limit $|q|/m_t \rightarrow 0$ with M_W related to the vev ⁷ by $2M_W = gv$. This limit corresponds to the “decoupling limit” where heavy quarks contribution to the QCD beta-function disappears, consistent with the discussion above for decoupling in the trace relation, (5.13). The effective

⁷Instead of v^{-1} , this can also be expressed in term of the Fermi coupling, G_F , where $\sqrt{2}G_F \equiv (g/2M_W)^2 = (1/v)^2$.

on-shell glueball-gluon-Higgs coupling, Γ_{GGH} , can now be obtained in this limit from (4.3) by taking the matrix element, $\Gamma_{GGH} \simeq \langle 0 | \int \mathcal{L} | \phi_H GG \rangle$. This corresponds to an effective replacement of $\langle G | t\bar{t} | G \rangle$ by $\langle G | F^2 | G \rangle$. To be more precise, we have

$$\begin{aligned} \Gamma_{GGH}(q^2) &\simeq \frac{gm_t}{2M_W} \langle G | t\bar{t} | G \rangle \simeq \frac{\alpha_s g}{24\pi M_W} \langle G | F_{\mu\nu}^a F^{a\mu\nu}(0) | G \rangle \\ &= \frac{\alpha_s g}{24\pi M_W} F_{GG}(q^2) \end{aligned} \quad (5.14)$$

with $q^2 = -m_H^2$. Eq. (5.10) serves to provide a normalization and continuation to physical q^2 can be done through (5.4). With m_H^2 large, this integral can be estimated by the ultra-local approximation discussed in Sec. (4.3). Observe that Γ_{GGH} has the dimension $O(E)$, as expected. Even more importantly, the only relevant mass scales are M_G^2 and the vev; the mass of Higgs does not enter. For more discussion on this point, see [1].

Since (5.8) plays a key role for our estimate for diffractive Higgs production, we provide below a more direct but equivalent derivation using Feynman-Hellman Theorem, without explicitly invoking trace-anomaly. All dimensionful quantities can be written in terms of Λ_{QCD} , or equivalently the glueball mass,

$$M_G(\alpha_s(\mu), \mu) = c_o \Lambda_{QCD} = c_o \mu e^{-\int^{\alpha_s(\mu)} \frac{d\alpha_s}{\alpha_s \beta}} \quad (5.15)$$

where ⁸

$$\frac{\mu}{\alpha_s} \frac{\partial \alpha_s}{\partial \mu} = 2\beta(\alpha_s)/g_s \equiv \tilde{\beta}(g) \quad (5.16)$$

Since masses must be independent of the choice of renormalization scheme, one has

$$0 = \mu \frac{d}{d\mu} M_G = M_G - \frac{\partial M_G}{\partial \alpha_s} \mu \frac{\partial \alpha_s}{\partial \mu} = M_G - \frac{M_G}{\tilde{\beta}(\alpha_s) \alpha_s} \mu \frac{\partial \alpha_s}{\partial \mu} \quad (5.17)$$

This is of course equivalent to

$$\alpha_s \frac{\partial}{\partial \alpha_s} M_G = -\frac{M_G}{\tilde{\beta}(\alpha_s)}. \quad (5.18)$$

Now we also can apply the Feynman-Hellman theorem to compute the derivative

$$1/\tilde{\beta}(\alpha_s) = -\alpha_s \frac{\partial \log M_G}{\partial \alpha_s} = -\frac{1}{16\pi\alpha_s} \frac{\langle G | G_{\mu\nu}^a G^{a\mu\nu}(0) | G \rangle}{M_G} \times \frac{V_3}{\langle G | G \rangle} \quad (5.19)$$

where the Hamiltonian has been taken in the form: $H = -(1/16\pi\alpha_s) \int_{V_3} d^3x G_{\mu\nu}^a G^{a\mu\nu} + \dots$. Taking the infinite volume limit $V_3 \rightarrow \infty$ and going back to the conventional normalization for the gauge field, one arrives at

$$\langle G | F_{\mu\nu}^a F^{a\mu\nu}(0) | G \rangle = -4\pi M_G^2 / 3\tilde{\beta}(\alpha_s) \quad (5.20)$$

as expected.

⁸The standard definition of the beta function give $\frac{\partial g}{\partial \mu} = \frac{g^3}{16\pi^2} [11N_c/3 - 2n_f/3] \rightarrow \frac{g^3}{16\pi^2} b$, with $b = 9$ for $N_c = 3, n_f = 3$. Here we use $\tilde{\beta}(g) = 2\beta(g)/g$.

5.3 Near-Forward limit

With the Higgs production vertex fixed by (5.11), all factors for the Higgs production amplitude, (4.26), are in principle determined, and we are now in the position to turn to the physical region where $t_1 \leq 0$ and $t_2 \leq 0$. To complete the discussion, let us examine here more closely the Pomeron kernel, leaving the phenomenological question of elastic vertex to the next section.

Consider first the elastic amplitude. In a strict supergravity limit, the kernel follows from a simple pole-dominance ansatz, Eq. (5.1), which is clearly inadequate at $t = 0$ since the amplitude remains real. However, with λ finite, as one moves from $t \simeq m_0^2$ to $t \simeq 0$, the amplitude becomes complex, with the leading s -dependence slowing down from s^2 to a non-integral power. To carry out this analysis, as we have explained earlier, it is necessary to revert to the J -plane representation, Eq. (3.6), for the Pomeron kernel $\tilde{\mathcal{K}}_P(s, t, z, z')$. When confinement deformation is implemented, the J -plane propagator $\tilde{G}_j(t, z, z')$ can be expressed generally in a spectral representation, (A.13). Equivalently, it can also be expressed as a sum of J -dependent poles in t , e.g., for hardwall model,

$$\tilde{G}_j(z, z'; t) = \sum_n \frac{\tilde{\phi}_n(z, j)\tilde{\phi}_n(z', j)}{m_n^2(j) - t}. \quad (5.21)$$

with $\tilde{\phi}_n(z, j)$ given in terms of Bessel functions. As one moves away from region near the tensor pole, the leading J -plane structure initially remains a Regge pole, As we move close to the $t = 0$ boundary, the J -plane structure is highly model-dependent. If asymptotic freedom is implemented, the amplitude remains meromorphic in J , and a leading pole approximation can remain meaningful. Realistically, due to diminishing trajectory spacings, a superposition of a large number of poles will be required. (See Appendix-A for more details.)

In what follows, we shall use the hardwall model as a guide. One finds the amplitude is dominated by a Regge pole initially in a region $m_1^2 < t < m_0^2$, where m_1^2 is the point where the leading pole disappears through the BPST cut at $j_0 = 2 - 2/\sqrt{\lambda}$, i.e., $m_0(j_0) = m_1$. As one further continues to the physical region where $t \leq 0$, the amplitude will now be dominated by the contribution from the BPST cut, with the inverse Mellin transform in J turning into an integral over the discontinuity across the cut. This leads to an explicit AdS representation for the Pomeron kernel in the near-forward limit,

$$\tilde{\mathcal{K}}_P(s, t, z, z') = \int_{-\infty}^{j_0} \frac{dj}{2\pi i} \xi(j) (\alpha' \hat{s})^j \text{Disc}_j \tilde{G}_j(t, z, z'). \quad (5.22)$$

Given the Pomeron kernel, both the elastic amplitude (2.5) and the diffractive central Higgs production amplitude, (4.25), are now completely specified, as promised.

For completeness, we note that analytic expression for the Pomeron kernel for the hard-wall model can be found in [11, 19], and it takes on a relatively simple form in the forward limit, i.e., at $t = 0$. For illustrative purpose, it is useful to exhibit its form in the conformal limit in an impact-representation. In this representation, one finds, for the imaginary part of the kernel [14],

$$\text{Im } \tilde{\mathcal{K}}_P = \frac{1}{\pi} \frac{1}{zz'} \frac{\xi}{\sinh \xi} (\sqrt{\lambda}/32\pi)^{1/2} e^{j_0 \tau} \frac{e^{-\sqrt{\lambda}\xi^2/2\tau}}{\tau^{3/2}}, \quad (5.23)$$

where $\tau = \log(\alpha'\hat{s})$, $e^\xi = 1 + v + \sqrt{v(2+v)}$, and v is the AdS_3 chordal distance squared, $v = (\mathbf{x}_\perp^2 + (z - z')^2)/2zz'$. While the above equation is given in impact parameter space, we can perform a Fourier transform to go to momentum space. This has a particularly simple form at $t = 0$, where the b -space integral can be performed explicitly to obtain

$$\text{Im } \tilde{\mathcal{K}}_P(s, 0, z, z') = \left(\frac{1}{8\pi\sqrt{\lambda}} \right)^{1/2} e^{j_0 \tau} \frac{\exp \left[-\frac{\sqrt{\lambda}}{2\tau} (\log z - \log z')^2 \right]}{\tau^{1/2}}, \quad (5.24)$$

which corresponds to a diffusion kernel in the AdS-radius. The imaginary part of the Pomeron kernel in the hardwall model similarly has a simple closed form expression at $t = 0$

$$\text{Im } \tilde{\mathcal{K}}_{HW}(s, 0, z, z') = \left(\frac{1}{8\pi\sqrt{\lambda}} \right)^{1/2} e^{j_0 \tau} \left(\frac{e^{-\frac{\sqrt{\lambda}}{2\tau} \log^2(z/z')}}{\tau^{1/2}} + F(z, z, \tau) \frac{e^{-\frac{\sqrt{\lambda}}{2\tau} \log^2(zz'/z_0^2)}}{\tau^{1/2}} \right). \quad (5.25)$$

The function

$$F(z, z', \tau) = 1 - 2\sqrt{\rho\pi\tau} e^{\eta^2} \text{erfc}(\eta), \quad \eta = \frac{-\log zz'/z_0^2 + 2\tau/\sqrt{\lambda}}{\sqrt{2\tau/\sqrt{\lambda}}}, \quad (5.26)$$

is fixed by the boundary conditions at z_0 , and it displays the relative strength of confinement. For a discussion, see [11, 19]. The real part of the kernel does not have a simple closed form expression, however it was shown in [14] that in the limit of large \hat{s} with λ large and fixed, so that $\sqrt{\lambda}/\log(\alpha'\hat{s}) \ll 1$, the relationship between the real and imaginary parts takes on a simple form

$$\text{Re } \tilde{\mathcal{K}}_P = \cot\left(\frac{\pi}{\sqrt{\lambda}}\right) \text{Im } \tilde{\mathcal{K}}_P. \quad (5.27)$$

5.4 First Estimate for Double-Pomeron Contribution

We now turn to a qualitative discussion for estimating the convolution over the AdS/QCD building blocks that determine Higgs production in our model. We emphasize however that in fact all the kernels are defined precisely through the differential equations and therefore with sufficient numerical effort can be computed directly once the explicit model AdS background is chosen

and the proton impact factor is fixed. This numerical step is premature and is postponed to a future phenomenological analysis.

Even to provide a rough phenomenological estimate for the central Higgs production cross section, we cannot avoid dealing with the coupling of Pomeron to the external protons. At present we are using a very naive model of the AdS proton. Below we treat the proton as a glueball wavefunction modified by a form factor for non-zero t . It is worth noting that an even simpler wave function, treating the proton as a “heavy” point like object at the IR cut-off, has already provided surprisingly good fits to the HERA DIS and DVCS data at small x . We anticipate the need to improve this in self-consistent fits. Indeed modeling the proton in the AdS context is an interesting topic in itself [42, 43, 44, 45, 46], as mentioned in the Introduction. As in the case of elastic scattering, it is also pedagogically reasonable to begin by first treating the simplest case of double-Pomeron exchange for Higgs production, i.e., without absorptive correction. Here, we discuss how phenomenologically reasonable simplifications can be made. This is followed by treating eikonal corrections in the next section, which provides a means of estimating the all-important survival probability.

It is often useful to make use of the conformal kernel at $t = 0$ [11, 14] where diffusion in the AdS radius is evident. The confinement can also be treated at $t = 0$, leading to (5.25). The structure of the kernel at $t < 0$, can in principle be obtained by solving the appropriate DE for the j -plane propagator. It can also be treated approximately, e.g., iteratively in an expansion about the known solution at $t = 0$. Alternatively, it is more useful to assume pole-dominance, e.g., keeping the contribution coming from a leading trajectory, even for t negative,

$$\tilde{G}_j(z, z'; t) \simeq \tilde{\phi}_{eff}(z, j) \frac{1}{m_{eff}^2(j) - t} \tilde{\phi}_{eff}(z', j). \quad (5.28)$$

where we approximate the BPST-cut contribution by that of an effective leading pole, with the Pomeron kernel behaving as $s^{j_{eff}(t)}$, where $j_{eff}(t)$, the trajectory function, determined by $m_{eff}^2(j(t)) = t$. That is, we assume $j_{eff}(t)$ remains real in the physical region where $t < 0$. By performing the inverse Mellin transform, (3.6), the large s -behavior of the BPST kernel can easily be obtained, leading to

$$A(s, t) \simeq g_{13}(t) \left(\frac{\xi(j_{eff}(t)) (\alpha' s)^{j_{eff}(t)}}{\alpha'^2 \tilde{m}^2(t)} \right) g_{24}(t) \quad (5.29)$$

where \tilde{m}^2 is the inverse of trajectory slope, $\tilde{m}^2(t) \equiv dm_{eff}^2(j(t))/dj$, and $\xi(j)$ is the signature factor. For the elastic amplitude, the coupling

$$g_{ij}(t) = \alpha' \int dz \sqrt{-g(z)} \Phi_{ij}(t, z) e^{-j_{eff}(t)A(z)} \tilde{\phi}_0(z, j_{eff}(t)) \quad (5.30)$$

is again in the form of an overlapping integral over the product of three wave functions, with $\tilde{\phi}_{eff} = \tilde{\phi}_0(z, j_{eff}(t))$. This serves as a continuation away from the on-shell spin-2 exchange by replacing the spin-2 wave function $\phi_G(z) = \tilde{\phi}_0(z, 2)$ by a corresponding wave function for a Pomeron, $\tilde{\phi}_0(z, j_{eff}(t))$, with spin shifted from 2 to $j_{eff}(t)$. Although this shift is of the order $O(1/\sqrt{\lambda})$, it is important to note that $\tilde{\phi}_0(z, j(t)) \sim z^{\Delta(j(t))-2}$, for $z \rightarrow 0$, in contrast to $\tilde{\phi}_0(z, 2) \sim z^2$. Note that we have continued with the convention where $g_{ij}(t)$ has the dimension of length. It is also easy to check ⁹ that (5.29) reduces to (5.1) as one approaches the tensor pole, $t \rightarrow m_0^2$.

Focussing next on the forward limit $t = 0$, we denote the effective intercept by \bar{j}_0 and inverse slope by \tilde{m}^2 . Together with the forward coupling $g_{ij}(0)$, they will be determined phenomenologically. We note that \tilde{m}^2 can be chosen to be of the order of the tensor glueball mass, m_0^2 . For consistency, we also assume that $\bar{j}_0 \simeq j_0$. In the high energy limit, $\xi(\bar{j}_0)$ provides the phase for the amplitude, with

$$|\xi|^2 = 1 + \rho^2 = 1 + \left(\frac{\text{Re } A(s, 0)}{\text{Im } A(s, 0)} \right)^2 \quad (5.31)$$

A corresponding treatment at $t_1 \simeq t_2 \simeq 0$ for the Higgs production amplitude, Eq. (4.25), can lead to a similar simplification. It follows, after a bit of algebra,

$$A(s, s_1, s_2, t_1 \simeq 0, t_2 \simeq 0) \simeq g_{13}(0) \frac{\xi(\bar{j}_0)^2 \Gamma_{PPH}(\alpha' s)^{\bar{j}_0}}{(\alpha' \tilde{m}^2)^2} g_{24}(0) \quad (5.32)$$

with an effective central vertex, related to $V_{PP\phi}$, (5.11), by

$$\Gamma_{PPH} \simeq \frac{\alpha_s g}{24\pi M_W} V_{PP\phi} (\alpha' m_H^2)^{\bar{j}_0} C(\bar{j}_0) \quad (5.33)$$

where

$$C(\bar{j}_0) = \int dz \sqrt{-g} e^{-4A(z)} \tilde{\phi}_0(z, \bar{j}_0) K(-m_H^2, z) \tilde{\phi}_0(z, \bar{j}_0) \quad (5.34)$$

and we have dropped terms lower order in $O(1/\sqrt{\lambda})$. We point out that (5.34) is finite due to the wave-function normalizability. For hard-wall, it is logarithmically divergent as $\bar{j}_0 \rightarrow j_0$ which corresponds to the onset of a Regge cut. In a proper treatment when the leading singularity is a cut, this apparent divergence will be absent. In order to avoid complicating the discussion, we proceed with the understanding that $C(\bar{j}_0)$ is of the order unity.

Let us turn next to the non-forward limit. We accept the fact that, in the physical region where $t < 0$ and small, the cross sections typically have an exponential form, with a logarithmic

⁹The tensor pole at $t = m_0^2$ is contained in the signature factor, and, in order to match (5.29) with (5.1) near $t = m_0^2$, a factor of $2/\pi$ has to be supplied. This can easily be absorbed, e.g., by a re-definition for the signature factor. We will not be concerned with such a re-definition for our present purpose.

slope which is mildly energy-dependent. We therefore approximate all amplitudes in the near forward region where $t < 0$ and small,

$$A(s, t) \simeq e^{B_{eff}(s) t/2} A(s, 0) \quad (5.35)$$

where $B_{eff}(s)$ is a smoothly slowly increasing function of s , (we expect it to be logarithmic). We also assume, for $t_1 < 0$, $t_2 < 0$ and small, the Higgs production amplitude is also strongly damped so that

$$A(s, s_1, s_2, t_1, t_2) \simeq e^{B'_{eff}(s_1) t_1/2} e^{B'_{eff}(s_2) t_2/2} A(s, s_1, s_2, t_1 \simeq 0, t_2 \simeq 0) \quad (5.36)$$

We also assume $B'_{eff}(s) \simeq B_{eff}(s) + b$. With these, both the elastic, the total pp cross sections and the Higgs production cross section can now be evaluated. Various cross sections will of course depend on the unknown slope parameter, B_{eff} , which can at best be estimated based on prior experience with diffractive estimates.

The phase space for diffractive Higgs production can be specified by the rapidity of Higgs y_H , and two-dimensional transverse momenta $q_{i,\perp}$, $i = 3, 4, 5$, with $q_{5,\perp} = q_{H,\perp}$, in a frame where the incoming momenta k_1 and k_2 are longitudinal. Alternatively, due to momentum conservation, we can use instead $y_H, t_1, t_2, \cos \phi$ as four independent variables where $t_1 \simeq -q_{3,\perp}^2$, $t_2 \simeq -q_{4,\perp}^2$, and $\cos \phi = \hat{q}_{3,\perp} \cdot \hat{q}_{4,\perp}$. However, the amplitude is effectively independent of ϕ since its dependence enters through the κ variable where $\kappa \simeq m_H^2 + q_{H,\perp}^2 = m_H^2 + (q_{2,\perp} + q_{4,\perp})^2$. As discussed earlier, for Higgs production, we can replace κ by $\kappa_{eff} \simeq m_H^2$.

Following the earlier analysis, Sec. 5.4, it is now possible to provide a first estimate for the double-diffractive Higgs production. It is possible to adopt an approach advocated by Kharzeev and Levin where the dependence on B_{eff} can be re-expressed in terms of other physical observables. Under our approximation, it is easy to show that the ratio $\sigma_{el}/\sigma_{total}^2$ can be expressed as

$$\frac{\sigma_{el}}{\sigma_{total}^2} = \frac{1 + \rho^2}{16\pi B_{eff}(s)} \quad (5.37)$$

where $\rho = \text{Re}A(s, 0)/\text{Im}A(s, 0)$. Upon squaring the amplitude, $A(s, s_1, s_2, t_1, t_2)$, (5.36), the double-differential cross section for Higgs production can now be obtained. After integrating over t_1 and t_2 and using the fact that, for m_H^2 large $s \simeq s_1 s_2 / m_H^2$, one finds

$$\frac{d\sigma}{dy_H} \simeq (1/\pi) \times C' \times |\Gamma_{GGH}(0)/\tilde{m}^2|^2 \times \frac{\sigma(s)}{\sigma(m_H^2)} \times R_{el}^2(m_H \sqrt{s}) \quad (5.38)$$

where $C' = (C(\bar{j}_0)/C)^2$. In this expression above, both C' and \tilde{m}^2 , like m_0^2 , are model dependent. It is nevertheless interesting to note that, since $\Gamma_{GGH}(0) \sim m_0^2$, the glueball mass scale also

drops out, leaving a model-dependent ratio of order unity. In deriving the result above, we have replaced B'_{eff} by B_{eff} where the difference is unimportant at high energy. With m_H in the range of $100GeV$, R_{el} can be taken to be in the range 0.1 to 0.2. For $C' \simeq 1$, $\tilde{m} \simeq m_0$, we find

$$\frac{d\sigma}{dy_H} \simeq .8 \sim 1.2 \text{ pbarn.} \quad (5.39)$$

This is of the same order as estimated in [1]. However, as also pointed in [1], this should be considered as an over-estimate. The major source of suppression will come from absorptive correction, which can lead to a central production cross section in the femtobarn range.

6 Summary and Discussion

There is of course already a growing literature with long historical roots applying both gluon perturbation theory and/or Regge parametrization to analyze diffractive processes. By extensive calibration with data, these are converging on estimates for double diffractive Higgs production [1, 2, 3, 4, 5, 6, 7, 8, 9, 10]. While there are still many areas of controversy in these models, a general agreement is the need to combine aspects of hard and soft scattering. These approaches can help us to gain further insight into the strong coupling approach and to guide future attempts to extract phenomenological constraints. The chief advantage of our holographic approach is the ability to unify both soft (Regge) and hard (BFKL) diffraction. When supplemented with the confinement deformation in AdS space, e.g., a hard-wall cutoff, our approach not only provides a description for the high energy near-forward scattering, but also allows one to analytically continue the amplitudes to tensor glueball pole to normalize the amplitude using the trace anomaly. Of course, as emphasized in the Introduction, we have but taken the first step in applying the BPST diffractive model for central Higgs production. What we have achieved so far is clearly not the final story, e.g., as for elastic amplitudes, it is well known that higher order contribution must be taken into account in order to restore the unitarity constraint.

There are also other considerations which we have glossed over in this initial effort. As stressed in the Introduction, the “bare-bone” double-Pomeron contribution to diffractive Higgs production requires three building blocks: the proton impact factors, Φ_{ij} and the Pomeron kernel (or Reggeon propagators), $\tilde{\mathcal{K}}_P$ and the Pomeron-Pomeron-Higgs vertex V_H . In this paper, we have treated the impact factors phenomenologically. In this concluding section, we focus on discussing how consideration of higher order contributions via an eikonal treatment leads to corrections for the central Higgs production. Following by now established usage, the resulting production cross section can be expressed in terms of a “survival probability” [63, 64, 65, 66, 67, 68, 69, 10]. In a more traditional usage, this eikonal sum can also be referred to as the “Good-Walker” sum [70], with contributions due to triple-Pomeron effect as coming from “enhanced diagrams”. For now, we shall ignore these complications and focus on the most important aspect which can be thought of as “local saturation” in the Euclidean AdS_3 .

The importance of eikonal correction can be seen as follows. One of the most important findings from String/Gauge duality is the fact that, at strong coupling, the single “Graviton” (Pomeron) exchange leads to an elastic amplitude which grows too fast, $\sim s^{j_0}$, with $j_0 \simeq 2 - O(1/\sqrt{\lambda})$. With the elastic amplitude growing as a power, it follows that that the dimensionless ratio R_{el} also grows asymptotically as s^{j_0-1} thus violating the constraint $R_{el} < 1$ and unitarity correction must be taken into account. Although the “bare Pomeron” approximation dominates

in the large N_c expansion, it is clear that higher order summations are necessary in order to restore unitarity. To go beyond the single-Pomeron approximation we must consider the high energy limit of lower order terms in the $1/N_c$ expansion. In flat space Veneziano has shown that higher closed string loops for graviton scattering eikonalize. Indeed in Refs. [13, 14] it was shown that the same sum leads to an eikonal expansion that exponentiates for each string bit frozen in impact parameter during the collision. To be more explicit, the resulting eikonal sum leads to an impact representation for the 2-to-2 amplitude

$$A(s, x^\perp - x'^\perp) = -2is \int dz dz' P_{13}(z) P_{24}(z') \left[e^{i\chi(s, x^\perp - x'^\perp, z, z')} - 1 \right] \quad (6.1)$$

The eikonal χ , as a function of $x_\perp - x'_\perp$, z, z' and s , can be determined by matching the first order term in χ to the single-Pomeron contribution, (2.5). In impact space representation, and one finds $\chi(s, x_\perp - x'_\perp, z, z') = \frac{g_0^2}{2s} \tilde{\mathcal{K}}_P(s, x_\perp - x'_\perp, z, z')$

This eikonal analysis can be extended directly to Higgs production. To simplify the discussion, we shall adopt a slightly formal treatment. Since Higgs is not part of the QCD dynamics, one can formally treat our eikonal as a functional of a weakly coupled external background Higgs field, $\phi_H(q^\pm, x_H^\perp, z_H)$, that is, in (6.1), we replace $A(s, x_\perp, x'_\perp)$ and $\chi(s, x^\perp - x'^\perp, z, z')$ by $A(s, x^\perp, x'^\perp; \phi_H)$ and $\chi(s, x^\perp - x'^\perp, z, z'; \phi_H)$, with the understanding that they reduce to $A(s, x_\perp, x'_\perp)$ and $\chi(s, x^\perp - x'^\perp, z, z')$ respectively in the limit $\phi_H \rightarrow 0$. Since Higgs production is a small effect, by expanding to first order in the Higgs background field, we find the leading order Higgs production amplitude, to all order in χ , becomes

$$\begin{aligned} A_H(s_1, s_2, x^\perp - x_H^\perp, x'^\perp - x_H^\perp, z_H) &= 2s \int dz dz' P_{13}(z) P_{24}(z') \\ &\times \chi_H(s_1, s_2, x^\perp - x_H^\perp, x'^\perp - x_H^\perp, z, z', z_H) e^{i\chi(s, x^\perp - x'^\perp, z, z')} \end{aligned} \quad (6.2)$$

where χ_H is given by the Higgs production amplitude, (4.25), due to double-Pomeron exchange in an impact representation¹⁰. The net effect of eikonal sum is to introduce a phase factor

$$e^{i\chi(s, x_\perp - x'_\perp, z, z')} = e^{i \operatorname{Re} \chi_R(s, x_\perp - x'_\perp, z, z')} e^{-\operatorname{Im} \chi(s, x_\perp - x'_\perp, z, z')} \quad (6.3)$$

into the production amplitude. Due to its absorptive part, $\operatorname{Im} \chi$, this eikonal factor provides a strong suppression for central Higgs production.

The effect of this suppression is often expressed in terms of a ‘‘Survival Probability’’, $\langle S \rangle$. In a momentum representation, the cross section for Higgs production per unit of rapidity

¹⁰To be more precise, up to a factor of $2s$, χ_H is given by matching $A_H(s, x_\perp, x'_\perp, \phi_H)$ at $|\chi| \ll 1$ with the integrand of (4.25) in an impact representation. We also note that here $s_1 s_2 / s \simeq m_H^2$. The kinematics of transverse AdS_3 coordinates is represented schematically in Fig. 5.

in the central region is

$$\frac{d\sigma_H(s, y_H)}{dy_H} = \frac{1}{\pi^3(16\pi)^2 s^2} \int d^2 q_{1\perp} d^2 q_{2\perp} |A_H(s, y_H, q_{1\perp}, q_{2\perp})|^2 \quad (6.4)$$

where y_H is the rapidity of the produced Higgs, $q_{1\perp}$ and $q_{2\perp}$ are transverse momenta of two outgoing fast leading particles in the frame where the momenta of incoming particles are longitudinal. In (6.4), we have skipped writing integrals over the AdS radial directions. ‘‘Survival Probability’’ is conventionally defined by the ratio

$$\langle S^2 \rangle \equiv \frac{\int d^2 q_{1\perp} d^2 q_{2\perp} |A_H(s, y_H, q_{1\perp}, q_{2\perp})|^2}{\int d^2 q_{1\perp} d^2 q_{2\perp} |A_H^{(0)}(s, y_H, q_{1\perp}, q_{2\perp})|^2} \quad (6.5)$$

where $A_H^{(0)}$ is the corresponding amplitude before eikonal suppression, e.g., given by Eq. (4.25). For simplicity, we shall also focus on the mid-rapidity production, i.e., $y_H \simeq 0$ in the overall CM frame. In this case, $\langle S^2 \rangle$ is a function of overall CM energy squared, s , or the equivalent total rapidity, $Y \simeq \log s$. Evaluating the survival probability as given by (6.5), though straight forward, is often tedious. The structure for both the numerator and the denominator is the same. For numerator factor, one has

$$\int dx_{\perp} dz d\bar{z} P_{13}(z) P_{13}(\bar{z}) \int dx'_{\perp} dz' d\bar{z}' P_{24}(z) P_{24}(z') \int e^{i(\chi(s, x_{\perp} - x'_{\perp}, z, z') - \chi^*(s, x_{\perp} - x'_{\perp}, \bar{z}, \bar{z}'))} \chi_H(s, s_1, s_2, x^{\perp} - x_H^{\perp}, x'^{\perp} - x_H^{\perp}, z, z') \chi_H^*(s, s_1, s_2, x^{\perp} - x_H^{\perp}, x'^{\perp} - x_H^{\perp}, \bar{z}, \bar{z}') \quad (6.6)$$

where we have made use of that fact that $z_H \simeq 1/m_H$. To obtain the denominator, one simply removes the phase factor, $e^{i(\chi(s, x_{\perp}, x'_{\perp}, z, z') - \chi^*(s, x_{\perp}, x'_{\perp}, \bar{z}, \bar{z}'))}$. It is now clear that it is this extra factor which controls the strength of suppression.

To gain a qualitative estimate, let us consider the local limit where $z \simeq \bar{z} \simeq z_0$ and $z' \simeq \bar{z}' \simeq z'_0$, with $z_0 \simeq z'_0 \simeq 1/\Lambda_{QCD}$. In this limit, one finds that this suppression factor reduces to

$$e^{-2 \text{Im} \chi(s, x_{\perp}, x'_{\perp}, z_0, z'_0)} \quad (6.7)$$

where $\text{Im} \chi > 0$ by unitarity. It follows that, in a super-gravity limit of strong coupling where the eikonal is strictly real, there will be no suppression and the survival probability is 1. Conversely, the fact that phenomenologically a small survival probability is required is another evidence that we need to work in an intermediate region where $1 < j_0 < 2$. In this more realistic limit, $\text{Im} \chi$ is large and cannot be neglected. In particular, it follows that the dominant region for diffractive Higgs production in pp scattering comes from the region where

$$\text{Im} \chi(s, x_{\perp} - x'_{\perp}, z, z') = O(1), \quad (6.8)$$

with $z \simeq z' = O(1/\Lambda_{QCD})$. Note that this is precisely the edge of the “disk region” for p-p scattering. In order to carry out a quantitative analysis, it is imperative that we learn the property of $\chi(s, \vec{b}, z)$ for $|\vec{b}|$ large. From our experience with pp scattering, DIS at HERA, etc., we know that confinement will play a crucial role. In pp scattering, since $z \simeq z' = O(1/\Lambda_{QCD})$, we expect this condition is reached at relatively low energy, as is the case for total cross section. It therefore plays a dominant role in determining the magnitude of diffractive Higgs production at LHC. We will not discuss this issue here further; more pertinent discussions on how to determine $\chi(s, x_\perp - x'_\perp, z, z')$ when confinement is important can be found in Ref. [19].

We end by re-iterating the importance of factorization, Eq. (1.4). Note that each separate factor in (1.4), up to a proportionality constant, can also be related to the amplitude of proton scattering off a heavy “onium” state, with a mass $O(m_H)$, or, equivalently, that for an off-shell Compton amplitude, e.g.,

$$\gamma^* (q_1) + \text{proton} (k_2) \rightarrow \gamma^* (q_3) + \text{proton} (k_4) \quad (6.9)$$

with $q_1^2 \simeq q_2^2 \simeq -m_H^2$. In this case, with t small, the photon is highly virtual and the amplitude can be thought of as a generalized DIS structure function, analogous to the “skewed unintegrated” parton distribution functions in a perturbative approach. (See, for instance, [71, 72, 73].) This will allow one to relate the double diffractive Higgs production amplitude to other measurables in DIS, after implementing some plausible assumptions [74, 75]. It is also worth noting that it should be possible to replace the internal vertex V_H , or equivalently replace the top quark loop by an operator for quark and anti-quark production at the boundary of AdS space and thus extend the AdS analysis to Pomeron fusion into heavy quark di-jets production, providing a powerful experimental test and calibration to the building blocks introduced for our diffractive Higgs production amplitude. We are considering how to do this but leave this extension as well as further phenomenological investigations to future research.

Acknowledgments: We are pleased to acknowledge useful conversations with M. Block, M. S. Costa, J. Ellis, E. Gotsman, H. Kowalski, E. Levin, U. Maor, D. A. Ross, M. Strassler, and C. Vergu. The work of R. C. B. was supported by the Department of Energy under contract DE-FG02-91ER40676, and that of C.-IT. by the Department of Energy under contract DE-FG02-91ER40688, Task-A. R.B. and C.-IT. would like to thank the Aspen Center for Physics for its hospitality during the early phase of this work. Centro de Física do Porto is partially funded by FCT and the work of M.D. is partially supported by grants PTDC/FIS/099293/2008 and CERN/FP/116358/2010 and by the FCT/Marie Curie Welcome II project.

References

- [1] D. Kharzeev and E. Levin, “Soft double-diffractive Higgs production at hadron colliders,” *Phys. Rev.* **D63** (2001) 073004, [hep-ph/0005311](#).
- [2] V. A. Khoze, A. D. Martin, and M. Ryskin, “The Rapidity gap Higgs signal at LHC,” *Phys.Lett.* **B401** (1997) 330–336, [hep-ph/9701419](#).
- [3] V. A. Khoze, A. D. Martin, and M. Ryskin, “Can the Higgs be seen in rapidity gap events at the Tevatron or the LHC?,” *Eur.Phys.J.* **C14** (2000) 525–534, [hep-ph/0002072](#).
- [4] M. Gay Ducati and G. Silveira, “Estimations for the Higgs boson production with QCD and EW corrections in exclusive events at the LHC,” *Phys.Rev.* **D84** (2011) 034042, [1104.3458](#).
- [5] R. Gastmans, S. L. Wu, and T. T. Wu, “Higgs production at the large hadron collider: Phenomenological model and theoretical predictions,” *Nucl.Phys.* **B850** (2011) 53–95.
- [6] A. Bialas and P. Landshoff, “Higgs production in pp collisions by double-pomeron exchange,” *Physics Letters B* **256** (1991), no. 34, 540 – 546.
- [7] T. Coughlin and J. Forshaw, “Central Exclusive Production in QCD,” *JHEP* **1001** (2010) 121, [0912.3280](#).
- [8] M. Spira, A. Djouadi, D. Graudenz, and P. Zerwas, “Higgs boson production at the LHC,” *Nucl.Phys.* **B453** (1995) 17–82, [hep-ph/9504378](#).
- [9] S. J. Brodsky, B. Kopeliovich, I. Schmidt, and J. Soffer, “Diffractive Higgs production from intrinsic heavy flavors in the proton,” *Phys.Rev.* **D73** (2006) 113005, [hep-ph/0603238](#).
- [10] M. Ryskin, A. Martin, and V. Khoze, “Soft processes at the LHC. II. Soft-hard factorization breaking and gap survival,” *Eur.Phys.J.* **C60** (2009) 265–272, [0812.2413](#).
- [11] R. C. Brower, J. Polchinski, M. J. Strassler, and C.-I. Tan, “The Pomeron and Gauge/String Duality,” *JHEP* **12** (2007) 005, [hep-th/0603115](#).
- [12] J. Polchinski and M. J. Strassler, “Deep inelastic scattering and gauge/string duality,” *JHEP* **05** (2003) 012, [hep-th/0209211](#).
- [13] R. C. Brower, M. J. Strassler, and C.-I. Tan, “On the Eikonal Approximation in AdS Space,” *JHEP* **03** (2009) 050, [0707.2408](#).

- [14] R. C. Brower, M. J. Strassler, and C.-I. Tan, “On The Pomeron at Large ’t Hooft Coupling,” *JHEP* **03** (2009) 092, 0710.4378.
- [15] L. Cornalba, M. S. Costa, J. Penedones, and R. Schiappa, “Eikonal approximation in AdS/CFT: Conformal partial waves and finite n four-point functions,” *Nucl. Phys.* **B767** (2007) 327–351, hep-th/0611123.
- [16] L. Cornalba, M. S. Costa, J. Penedones, and R. Schiappa, “Eikonal approximation in AdS/CFT: From shock waves to four- point functions,” hep-th/0611122.
- [17] L. Cornalba, “Eikonal Methods in AdS/CFT: Regge Theory and Multi-Reggeon Exchange,” 0710.5480.
- [18] L. Cornalba, M. S. Costa, and J. Penedones, “Eikonal Approximation in AdS/CFT: Resumming the Gravitational Loop Expansion,” *JHEP* **09** (2007) 037, 0707.0120.
- [19] R. C. Brower, M. Djuric, I. Sarcevic, and C.-I. Tan, “String-Gauge Dual Description of Deep Inelastic Scattering at Small- x ,” *JHEP* **11** (2010) 051, 1007.2259.
- [20] M. S. Costa and M. Djuric, “Deeply Virtual Compton Scattering from Gauge/Gravity Duality,” 1201.1307.
- [21] L. Cornalba and M. S. Costa, “Saturation in Deep Inelastic Scattering from AdS/CFT,” *Phys. Rev.* **D78** (2008) 096010, 0804.1562.
- [22] L. Cornalba, M. S. Costa, and J. Penedones, “AdS black disk model for small- x DIS,” *Phys. Rev. Lett.* **105** (2010) 072003, 1001.1157.
- [23] C. P. Herzog, S. Paik, M. J. Strassler, and E. G. Thompson, “Holographic Double Diffractive Scattering,” *JHEP* **08** (2008) 010, 0806.0181.
- [24] S. Hong, S. Yoon, and M. J. Strassler, “On the couplings of the rho meson in AdS/QCD,” hep-ph/0501197.
- [25] S. Hong, S. Yoon, and M. J. Strassler, “On the couplings of vector mesons in AdS/QCD,” *JHEP* **04** (2006) 003, hep-th/0409118.
- [26] E. Witten, “Anti-de Sitter space and holography,” *Adv. Theor. Math. Phys.* **2** (1998) 253–291, hep-th/9802150.
- [27] S. S. Gubser, I. R. Klebanov, and A. M. Polyakov, “Gauge theory correlators from non-critical string theory,” *Phys. Lett.* **B428** (1998) 105–114, hep-th/9802109.

- [28] V. Balasubramanian, P. Kraus, and A. E. Lawrence, “Bulk vs. boundary dynamics in anti-de Sitter spacetime,” *Phys. Rev.* **D59** (1999) 046003, [hep-th/9805171](#).
- [29] T. Banks, M. R. Douglas, G. T. Horowitz, and E. J. Martinec, “AdS dynamics from conformal field theory,” [hep-th/9808016](#).
- [30] I. R. Klebanov and E. Witten, “AdS/CFT correspondence and symmetry breaking,” *Nucl. Phys.* **B556** (1999) 89–114, [hep-th/9905104](#).
- [31] J. Polchinski and M. J. Strassler, “The string dual of a confining four-dimensional gauge theory,” [hep-th/0003136](#).
- [32] K. Skenderis, “Lecture notes on holographic renormalization,” *Class. Quant. Grav.* **19** (2002) 5849–5876, [hep-th/0209067](#).
- [33] R. C. Brower, M. Djuric, and C.-I. Tan, “Odderon in gauge/string duality,” *JHEP* **07** (2009) 063, [0812.0354](#).
- [34] A. Donnachie and P. V. Landshoff, “Total Cross-Sections,” *Phys. Lett.* **B296** (1992) 227–232, [hep-ph/9209205](#).
- [35] A. Donnachie and P. V. Landshoff, “Small x: Two pomerons!,” *Phys. Lett.* **B437** (1998) 408–416, [hep-ph/9806344](#).
- [36] A. Capella, U. Sukhatme, C.-I. Tan, and J. Tran Thanh Van, “Dual parton model,” *Phys. Rept.* **236** (1994) 225–329.
- [37] V. S. Fadin, E. A. Kuraev, and L. N. Lipatov, “On the Pomeranchuk Singularity in Asymptotically Free Theories,” *Phys. Lett.* **B60** (1975) 50–52.
- [38] E. A. Kuraev, L. N. Lipatov, and V. S. Fadin, “Multi - Reggeon Processes in the Yang-Mills Theory,” *Sov. Phys. JETP* **44** (1976) 443–450.
- [39] E. A. Kuraev, L. N. Lipatov, and V. S. Fadin, “The Pomeranchuk Singularity in Nonabelian Gauge Theories,” *Sov. Phys. JETP* **45** (1977) 199–204.
- [40] I. I. Balitsky and L. N. Lipatov, “The Pomeranchuk Singularity in Quantum Chromodynamics,” *Sov. J. Nucl. Phys.* **28** (1978) 822–829.
- [41] A. D. Martin, M. G. Ryskin, and V. A. Khoze, “From hard to soft high-energy pp interactions,” [1110.1973](#).
- [42] K. Hashimoto, N. Iizuka, and P. Yi, “A Matrix Model for Baryons and Nuclear Forces,” *JHEP* **10** (2010) 003, [1003.4988](#).

- [43] K. Hashimoto, T. Sakai, and S. Sugimoto, “Holographic Baryons : Static Properties and Form Factors from Gauge/String Duality,” *Prog. Theor. Phys.* **120** (2008) 1093–1137, 0806.3122.
- [44] P. Yi, “A holographic QCD and baryons from string theory,” *Prog. Theor. Phys. Suppl.* **177** (2009) 247–261.
- [45] S. K. Domokos, J. A. Harvey, and N. Mann, “Setting the scale of the p p and p bar p total cross sections using AdS/QCD,” *Phys. Rev.* **D82** (2010) 106007, 1008.2963.
- [46] S. K. Domokos, J. A. Harvey, and N. Mann, “The Pomeron contribution to p p and p bar p scattering in AdS/QCD,” *Phys. Rev.* **D80** (2009) 126015, 0907.1084.
- [47] J. Polchinski and M. J. Strassler, “Hard scattering and gauge / string duality,” *Phys. Rev. Lett.* **88** (2002) 031601, hep-th/0109174.
- [48] C. Csaki, M. Reece, and J. Terning, “The AdS/QCD Correspondence: Still Undelivered,” *JHEP* **05** (2009) 067, 0811.3001.
- [49] C. Csaki and M. Reece, “Toward a systematic holographic QCD: A braneless approach,” *JHEP* **05** (2007) 062, hep-ph/0608266.
- [50] A. Karch, E. Katz, D. T. Son, and M. A. Stephanov, “Linear Confinement and AdS/QCD,” *Phys. Rev.* **D74** (2006) 015005, hep-ph/0602229.
- [51] J. Erlich, E. Katz, D. T. Son, and M. A. Stephanov, “QCD and a Holographic Model of Hadrons,” *Phys. Rev. Lett.* **95** (2005) 261602, hep-ph/0501128.
- [52] G. F. de Teramond and S. J. Brodsky, “Light-Front Quantization and AdS/QCD: An Overview,” 1103.1100.
- [53] A. D. Martin, M. G. Ryskin, and V. A. Khoze, “Soft physics and exclusive Higgs production at the LHC,”. Prepared for London Workshop on Standard Model discoveries with early LHC data, London, England, 30 Mar - 1 Apr 2009.
- [54] R. C. Brower, C. E. DeTar, and J. H. Weis, “Regge Theory for Multiparticle Amplitudes,” *Phys. Rept.* **14** (1974) 257.
- [55] F. Englert and R. Brout, “Broken Symmetry and the Mass of Gauge Vector Mesons,” *Phys.Rev.Lett.* **13** (1964) 321–322.
- [56] P. W. Higgs, “Broken Symmetries and the Masses of Gauge Bosons,” *Phys.Rev.Lett.* **13** (1964) 508–509.

- [57] G. Guralnik, C. Hagen, and T. Kibble, “Global Conservation Laws and Massless Particles,” *Phys.Rev.Lett.* **13** (1964) 585–587.
- [58] G. S. Guralnik, “Gauge Invariance and the Goldstone Theorem,” *Mod.Phys.Lett.* **A26** (2011) 1381–1392, 1107.4592.
- [59] P. W. Higgs, “Spontaneous Symmetry Breakdown without Massless Bosons,” *Phys.Rev.* **145** (1966) 1156–1163.
- [60] J. F. Gunion, H. E. Haber, G. L. Kane, and S. Dawson, “THE HIGGS HUNTER’S GUIDE,” *Front. Phys.* **80** (2000) 1–448.
- [61] R. C. Brower, H. Nastase, H. J. Schnitzer, and C.-I. Tan, “Analyticity for Multi-Regge Limits of the Bern-Dixon- Smirnov Amplitudes,” *Nucl. Phys.* **B822** (2009) 301–347, 0809.1632.
- [62] R. C. Brower, S. D. Mathur, and C.-I. Tan, “Glueball Spectrum for QCD from AdS Supergravity Duality,” *Nucl. Phys.* **B587** (2000) 249–276, hep-th/0003115.
- [63] J. D. Bjorken, “Rapidity gaps and jets as a new-physics signature in very-high-energy hadron-hadron collisions,” *Phys. Rev. D* **47** (Jan, 1993) 101–113.
- [64] E. Gotsman, E. Levin, and U. Maor, “Large rapidity gaps in p p collisions,” *Phys.Lett.* **B309** (1993) 199–204, hep-ph/9302248.
- [65] E. Gotsman, E. Levin, and U. Maor, “The Survival probability of large rapidity gaps in a three channel model,” *Phys.Rev.* **D60** (1999) 094011, hep-ph/9902294.
- [66] E. Gotsman, E. Levin, U. Maor, and J. Miller, “A QCD motivated model for soft interactions at high energies,” *Eur.Phys.J.* **C57** (2008) 689–709, 0805.2799.
- [67] E. Gotsman, E. Levin, and U. Maor, “Survival probability of large rapidity gaps in QCD and N=4 SYM motivated model,” *Eur.Phys.J.* **C71** (2011) 1685, 1101.5816.
- [68] A. Kaidalov, V. A. Khoze, A. D. Martin, and M. Ryskin, “Probabilities of rapidity gaps in high-energy interactions,” *Eur.Phys.J.* **C21** (2001) 521–529, hep-ph/0105145.
- [69] M. Ryskin, A. Martin, and V. Khoze, “Soft diffraction at the LHC: A Partonic interpretation,” *Eur.Phys.J.* **C54** (2008) 199–217, 0710.2494.
- [70] M. Good and W. Walker, “Diffraction dissociation of beam particles,” *Phys.Rev.* **120** (1960) 1857–1860.

- [71] X.-D. Ji, “Gauge invariant decomposition of nucleon spin,” *Phys. Rev. Lett.* **78** (1997) 610–613, [hep-ph/9603249](#).
- [72] X.-D. Ji, “Deeply-virtual Compton scattering,” *Phys. Rev.* **D55** (1997) 7114–7125, [hep-ph/9609381](#).
- [73] X.-D. Ji, “Off-forward parton distributions,” *J. Phys.* **G24** (1998) 1181–1205, [hep-ph/9807358](#).
- [74] J. Ellis, H. Kowalski, and D. A. Ross, “Evidence for the Discrete Asymptotically-Free BFKL Pomeron from HERA Data,” *Phys. Lett.* **B668** (2008) 51–56, [0803.0258](#).
- [75] D. A. Ross, H. Kowalski, L. N. Lipatov, and G. Watt, “Low-x gluon distribution from a discrete version of the BFKL pomeron,” *AIP Conf. Proc.* **1350** (2011) 47–50.
- [76] A. Hashimoto and Y. Oz, “Aspects of QCD dynamics from string theory,” *Nucl. Phys.* **B548** (1999) 167–179, [hep-th/9809106](#).
- [77] O. DeWolfe, D. Z. Freedman, S. S. Gubser, and A. Karch, “Modeling the fifth dimension with scalars and gravity,” *Phys. Rev.* **D62** (2000) 046008, [hep-th/9909134](#).

A AdS QCD and Conformal Symmetry Breaking

In this appendix, we first present a model with scale invariance breaking due to confinement deformation, leading to non-vanishing expectation values for $\langle F^2 \rangle$, etc. Under such a condition, there will be a Witten graviton-graviton-dilaton vertex in the bulk as well as the existence of tensor glueballs. We next turn to a more amenable model, e.g., the hard-wall model, where, due to confinement, the existence of a tensor glueball can be more easily studied. This approach can also be used to provide a more explicit representation for our Pomeron kernel, \mathcal{K}_P . Lastly, we discuss consequence of asymptotic freedom, and point out how a non-vanishing beta-function can be used to relate gluon condensate to the non-vanishing trace for the energy-momentum tensor. This observation has been used to provide an estimate on the magnitude for the central Higgs production vertex V_H in Sec. 5.

Symmetry Breaking and AdS/CFT Correspondence: Symmetry breaking effect has been studied in AdS/CFT correspondence mostly using a near-boundary analysis [26, 27, 28, 29, 30, 31, 32]. In a standard AdS/CFT treatment for $d = 4$, $\mathcal{N} = 4$ Yang-Mills theory, each local operator \mathcal{O}_i of dimension Δ_i in the CFT corresponds to two possible solutions of the linearized field equations for an associated bulk field Φ_i near the *AdS* boundary [26, 27], a nonnormalizable solution which scales with the AdS radius as r^{Δ_i-4} with r the *AdS* radius, and a normalizable solution which scales as $r^{-\Delta_i}$. As explained carefully in [31], when a CFT is perturbed by a symmetry breaking local operator $a_i \mathcal{O}_i$, a non-vanishing vev $\langle \mathcal{O}_i \rangle$ corresponds to a supergravity solution which behaves at large r as

$$a_i r^{\Delta_i-4} + \dots + b_i r^{-\Delta_i} + \dots \tag{A.1}$$

where $\langle \mathcal{O}_i \rangle = b_i$. For our present purpose, it is more profitable to address scale invariance braking in terms of Witten diagrams in the bulk.

In a truly realistic treatment of QCD, one expects scale invariance breaking due to running of QCD coupling, with the trace of the stress-energy tensor related to F^2 by the QCD beta-function, e.g., $\langle T_\mu^\mu \rangle = \beta \langle F^2 \rangle$. In an approximate treatment where conformal invariance is maintained, on the other hand, it follows that $T_{\mu\nu}$ remains traceless, with vanishing $\langle F^2 \rangle = 0$, etc. More generally, we will be interested in n-point correlators involving F^2 and $T_{\mu\nu}$, which can be evaluated at strong coupling through the use of Witten diagrams. Under such a scenario, as we shall explain below by an explicit model for dilaton-gravity, the relevant Graviton-Higgs-Graviton coupling in the bulk would vanish. That is, there would be no double diffractive Higgs production at strong coupling! Fortunately, in a framework with proper confinement

deformation, scale invariance is broken with non-vanishing vev for F^2 , and the Graviton-Higgs-Graviton coupling is non-zero. Furthermore, when the running coupling is properly taken into account, through the conformal anomaly, we are able to fix the normalization of double diffractive Higgs production.

Central Vertex and Scale Invariance Breaking: The importance of scale invariance breaking for the QCD dynamics has been emphasized in [76]. It has also been discussed by many in connection with the spectrum of light scalar glueballs. It is possible to adopt a holographic approach where one couples 5d gravity to a dilaton with AdS_5 geometry in the UV, Eq. (2.2) while taking on a non-trivial background. For instance, this can be achieved by considering a toy model with action [49]

$$S = M_P^2 \int d^5x \sqrt{g} \left(-\mathcal{R} - V(\phi) + \frac{1}{2} g^{MN} \partial_M \phi \partial_N \phi - \lambda(\phi) T(z) \right) \quad (\text{A.2})$$

where ϕ is the dilaton and $V(\phi)$ is a dilatonic potential and we have added an external “brane” source. This system was analyzed in some detail in DeWolfe, Freedman, Gubser and Karch [77] by mapping the problem into the solution of a super potential. A first question is, without introducing an external brane source, but with a potential V appropriately chosen, is it possible to simulate running coupling, scale invariance breaking, etc? This leads to a non-vanishing gluon condensate, and, in such a setting, a non-vanishing graviton-graviton-dilaton vertex can be obtained. Since double diffractive Higgs production proceeds via scalar glueball production, as discussed earlier, this in turn leads to a non-vanishing Pomeron-Pomeron-Higgs vertex, V_H .

Consider first an example leading to a “near- AdS ” geometry, (2.2), by having a dilaton background, $\phi_{cl}(z)$, which can be non-trivial. Expanding the action about this background, $G_{mn} = g_{mn} + h_{mn}$ and $\phi = \phi_{cl} + \varphi$, and consider traceless-transverse h_{mn} appropriate for Pomeron/Graviton fluctuations, terms linear in h and φ vanish, quadratic terms serve to determine the glueball spectrum, and higher order terms correspond to couplings in a Witten diagrammatic treatment. We are therefore interested in a term linear in φ and quadratic in h . Expanding the action we obtain terms of this order

$$S_{int} = \frac{M_P^2}{4} \int dz d^4x \sqrt{-g} h^{nm} h_{mn} [V'(\phi_{cl})\varphi - g^{zz} \partial_z \phi_{cl}(z) \partial_z \varphi]. \quad (\text{A.3})$$

where $\phi_{cl}(z)$ is the classical background. Note in the pure AdS^5 conformal background, the potential is a constant, $V = -12/R^2$, i.e., it simply provides the cosmological constant, and $\phi_{cl}(z) = \text{const}$. It follows both terms above are zero. That is, the graviton-graviton-dilaton coupling vanishes identically in a conformal limit.

Conversely, if the background is non-trivial, and breaks scale invariance, a more involved potential $V(\phi)$ is required. This in turn leads to a non-zero graviton-graviton-dilaton coupling. This can best be illustrated for example by the special “subcritical asymptotically free” solution, discussed in Csaki et al. [49], where

$$V(\phi) = -\frac{6}{R^2}e^{\sqrt{2/3}\phi} - \frac{12}{R^2} \quad , \quad \phi_{cl} = -\sqrt{3/2} \log \log(z_0/z) \quad (\text{A.4})$$

We note that, for this case,

$$e^{\sqrt{2/3}\phi_{cl}} = 1/\log(z_0/z) \quad (\text{A.5})$$

As an illustration of the effects of running coupling in the UV, this model gives

$$S_{int} = -\frac{M_P^2}{4} \int dz d^4x \sqrt{-g} \frac{\sqrt{6}}{R^2 \log(z_0/z)} h^{nm} h_{mn} [\phi + \frac{z}{4} \partial_z \phi] \quad (\text{A.6})$$

with a non-trivial graviton-graviton-dilaton coupling in the bulk.

Although the model discussed above looks attractive, it nevertheless cannot serve as a realistic model for QCD as we will indicate shortly. The precise choice of the best background is therefore left to future phenomenology. Here it is sufficient to assume that there is confining background so that there is a stable (at large N) tensor glueball on the leading trajectory at $J = 2$ and a non-zero Pomeron-Pomeron-dilaton vertex. As we shall see shortly, the existence of a tensor glueball plays a crucial role in our treatment, we turn next to a more detailed analysis using a hard-wall background which is also more amenable to a J -plane analysis, necessary for discussing our Pomeron kernel.

Tensor Glueballs and Confinement Deformation: Let us begin by first considering confinement deformations keeping the ultraviolet region conformal. If confinement sets in at a scale Λ in the gauge theory, this leads to a change in the metric away from AdS_5 in the region near $z = R^2/r \sim 1/\Lambda = z_0$. One can think of the space being “cut-off” or “rounded off”, in some natural way at $z = z_0$, leading to a “wave-guide” effect. This in general leads to a theory with a discrete hadron spectrum, with mass splitting of the order Λ among hadrons of spin ≤ 2 . As discussed in [11], the differential operator determining the J -plane spectrum remains approximately unaffected for $-t \gg \Lambda^2$, while the effect of confinement becomes important as $t \rightarrow 0^-$, and for any $t > 0$. To gain a qualitative understanding, it is instructive to treat below the “hard-wall” model, so that Eq. (3.7) remains valid, with z cutoff in the range $[0, z_0]$. While this model is not a fully consistent theory, it does capture key features of confining theories with string theoretic dual descriptions.

To set the proper stage, let us first review the situation in the conformal limit. Recall that, at finite λ , it has been shown in Ref. [11] that, due to curvature of AdS, the effective spin of a graviton exchange is lowered from 2 to $j_0 = 2 - 2/\sqrt{\lambda}$. As such it is necessary to adopt a J -plane formalism where the Pomeron kernel $\tilde{\mathcal{K}}_P$ is given by an inverse Mellin transform,

$$\tilde{\mathcal{K}}_P(s, t, z, z') = - \int_{-i\infty}^{i\infty} \frac{dj}{2\pi i} (\alpha' \hat{s})^j \frac{1 + e^{-i\pi j}}{\sin \pi j} \tilde{G}_j(t, z, z'). \quad (\text{A.7})$$

with $\hat{s} = zz's/R^2$. Note that the $J = 2$ contribution is

$$(2/\pi)(\alpha' \hat{s})^2 \tilde{G}_2(t, z, z'). \quad (\text{A.8})$$

This is simply the graviton Kernel, (3.3), up to a constant factor, which can be absorbed into the coupling. When conformal invariance is maintained, this J -dependent propagator $\tilde{G}_j(t, z, z')$ satisfies the standard AdS_5 differential equation

$$\left(-z\partial_z z\partial_z + (2\sqrt{\lambda})(j - j_0) - z^2 t\right) \tilde{G}_j(z, z'; t) = z \delta(z - z') \quad (\text{A.9})$$

with $j_0 = 2 - 2/\sqrt{\lambda}$. This equation can also be expressed in a standard Schrodinger form. It can be solved either by a spectral resolution in t or in j . Holding $j > j_0$ first and real, the spectrum in t can be seen to be continuous, along its positive real axis, leading to

$$\tilde{G}_j(z, z'; t) = \int_0^\infty k dk \frac{J_{(\Delta(j)-2)}(kz) J_{(\Delta(j)-2)}(kz')}{k^2 - t}. \quad (\text{A.10})$$

where $\Delta(j) = 2 + \sqrt{2\sqrt{\lambda}(j - j_0)}$. If, on the other hand, an IR hard-wall cutoff is introduced, the spectrum in t becomes discrete. The propagator is now given by a discrete sum,

$$\tilde{G}_j(z, z'; t) = \sum_n \frac{\tilde{\phi}_n(z, j) \tilde{\phi}_n(z', j)}{m_n^2(j) - t}. \quad (\text{A.11})$$

The wave-functions $\tilde{\phi}_n(z, j)$ can again be expressed in terms of Bessel functions, with $m_n(j)$ fixed by a Neumann condition at z_0 , $[z^j \tilde{\phi}_n(z, j)]'|_{z=z_0} = 0$. This discrete structure is what is to be expected when confinement deformation is introduced.

Alternatively, one finds that

$$\tilde{G}_j(z, z'; t) = \int_{-\infty}^{\infty} \frac{d\nu}{\pi^2} (\nu \sinh \pi\nu) \frac{K_{i\nu}(qz) K_{i\nu}(qz')}{2\sqrt{\lambda}(j - j_0) + \nu^2} \quad (\text{A.12})$$

where $t = -q^2 < 0$. (A.12) provides a different representation for the Pomeron propagator in the conformal limit. One observes more directly the presence of the branch cut at $j = j_0$, which corresponds to the minimum of the denominator in (A.12). From (A.10), the presence of this

cut has to be inferred from the dependence through $\Delta(j)$. Equivalently, one can work directly with a spectrum analysis in the J -plane, as carried out in Ref. [14]. The analysis can best be thought of as working with the boost operator, $\hat{H} = M_{+-}$, which is conjugate to J .

It is also just as easy to treat the problem more generally, e.g., with $e^{-2A(z)}$ replacing $(R/z)^2$ as a confining warping factor. The Green's function is the spectral representation for the operator, $(j - \hat{H})^{-1}$,

$$G_j(q_\perp, z, z') = e^{-jA(z)} \sum_n \frac{\psi_n(q_\perp, z)\psi_n(q_\perp, z')}{j - \lambda_n(q)} e^{-jA(z')} \quad (\text{A.13})$$

where traditional one regards $\omega_n = \lambda_n - 1$ as eigen-energies of boost operator ¹¹.

Further discussion on these construct can be found in Ref. [11]. Here, we simply display in Fig. 7, the structure of these Regge singularity for J and t real. In particular, we emphasize that, when the trajectory crosses $j = 2$, it corresponds to a physical tensor glueball. This important feature we shall make use of in the next section.

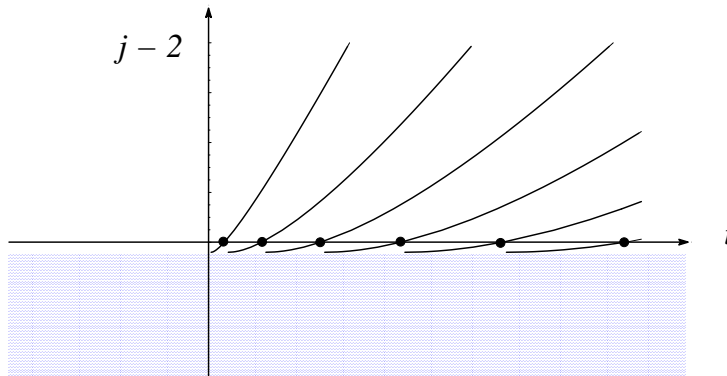


Figure 7: The analytic behavior of Regge trajectories in the hard-wall model, showing the location of the bound-state poles at $j = 2$ and the t -independent continuum cut (shaded) at $j = j_0 = 2 - 2/\sqrt{\lambda}$ into which the Regge trajectories disappear. The lowest Regge trajectory intersects the cut at a small positive value of t . At sufficiently large t each trajectory attains a fixed slope, corresponding to the tension of the model's confining flux tubes.

It is possible to adopt a more general background which mimics the features of running coupling. This has also been done in [11]. The result is a discrete spectrum in the Regge plane in agreement with expectation based on asymptotic freedom for the BRST equation, Fig. 8.

¹¹Actually confinement alone has both a discrete and continuum spectrum, which we do not exhibit explicitly here.

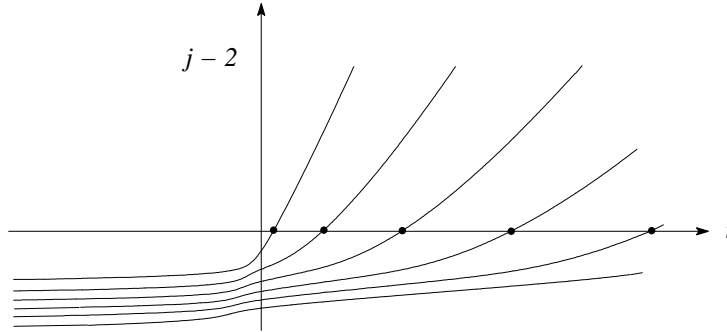


Figure 8: Discrete Regge Spectrum at negative t due to running coupling

Modeling Asymptotic Freedom and Broken Scale Invariance: In a realistic holographic treatment of QCD, asymptotic freedom must be handled consistently. Although there have been several models to implement some features of running coupling [11, 49], they nevertheless do not prove to be entirely inadequate. For instance, they fail to give the correct running coupling dependence as measured by the potential between static quarks at a small separation L

$$V_{\bar{Q}Q}(L) \simeq -\alpha(L)/L \quad , \quad \alpha(L) = \frac{g^2 N_c}{-\log(\mu L)} \quad (\text{A.14})$$

when computed using the Nambu action in these deformed backgrounds. We have checked that the background of [49] with running coupling does not support this interpretation. An analogous suggestion in [11], discussed briefly above, does lead closer to the desired answer. However it is not a solution to pure dilaton gravity. It requires a negative tension brane in the UV to support it or some other source of energy. Perhaps it is not surprising that to wed the UV behavior to a smooth effective background at strong coupling should be difficult. A real QCD dual theory would have to describe hard scattering and gluon jets at high energy not just a running coupling. Most likely this at the very least implies highly curved background far from these phenomenological attempts.

Clearly the details of such a construct go beyond the scope of the current discussion. It suffices to emphasize that $V_H \neq 0$ is a general consequence of scale anomaly. As pointed out earlier, in a naive application of the hard-wall model, such vertex is indeed absent in the bulk. Therefore, our discussion of Higgs production in AdS/CFT should be understood in a more general setting with a proper confinement deformation of the AdS geometry.